Utrecht University

Faculty of Veterinary Medicine

The Role of Parathyroid hormone-related peptide and Indian Hedgehog in Intervertebral Disc Degeneration

---

Department of Clinical Sciences of Companion Animals, Faculty of Veterinary Medicine, Utrecht University, June 2017

Master Research Internship and Track

K.M. de Rooij
Solis-ID: 3779971
Daily supervisor: Drs. F.C. Bach
Principal investigator: Dr. M.A. Tryfonidou

Table of Contents

1. Abstract

Introduction - The vertebral column consists of vertebrae interconnected by intervertebral discs (IVDs). Each IVD consists of a central nucleus pulposus (NP) and an outer annulus fibrosus (AF). IVDs provide movement, flexibility and stability of the vertebral column. IVD degeneration is common in humans and dogs, and is associated with low back pain. Current treatments reduce the pain rather than repair the IVD. Therefore, regenerative treatments need to be developed, but further knowledge about the pathogenesis of IVD degeneration and the pathways involved is required. The Parathyroid hormone-related peptide (PTHrP) and Indian Hedgehog (IHH) growth-restraining feedback loop plays an essential role in endochondral ossification. IHH may be positively correlated with osteoarthritis, which resembles IVD degeneration. Additionally, IHH promotes chondrocyte hypertrophy and mineralization, while PTHrP suppresses these processes which also occur during IVD degeneration. The aim of this study was to determine the expression and possible role of PTHrP and IHH in canine and human healthy and degenerated IVDs.

Methods – Human and canine IVDs with different Thompson grades were immunohistochemically stained for PTHrP, IHH, PTHR1, Ptc and Smo. The mean ratio of positive cells per Thompson grade was assessed in the NP. Additionally, nucleus pulposus cells (NPCs) from early degenerated human and canine IVDs (Thompson grade III) were cultured in 3D micro-aggregates in chondrogenic differentiation culture medium (10 ng/mL TGF-ß$_1$), or hypertrophic induction medium (1 nM triiodothyronine, 10 mM ß-glycerol phosphate and 10^{-9} M dexamethasone), or hypertrophic induction medium supplemented with PTHrP (10^{-8} M or 10^{-7}M) or IHH (0.1 µg/mL or 1 µg/mL) in hypoxia and normoxia. Read out parameters were ECM production (RT-qPCR, glycosaminoglycan (GAG) production, Safranin O/Fast Green staining, immunohistochemistry) and cell proliferation (RT-qPCR, DNA content).

Results – Generally, in canines and humans, PTHrP and IHH (and its receptors Ptc and Smo) protein expression decreased from healthy to early degenerated IVDs and increased from early to severely degenerated IVDs. Collagen type X protein expression or calcifications, which are hypertrophic markers, were not present in the NPCs that were treated with hypertrophic induction medium. However, PTHR1 protein expression, which is a prehypertrophic marker, was present. The protein PTHR1 was more strongly expressed in the canine NPCs that were cultured in normoxia than it was in hypoxia. In normoxia, PTHR1 was most strongly expressed in canine NPCs that were treated with hypertrophic induction medium for 21 days. Supplementation with PTHrP or IHH did not augment GAG production in the hypertrophic NPCs. Calcifications were visible in one canine and one human donor that were treated with hypertrophic induction medium supplemented with 1 µg/mL IHH.

Conclusions – This study demonstrated that both PTHrP and IHH positively correlate with the IVD degeneration grade in humans. This indicates that PTHrP-IHH signaling is active in healthy and degenerated IVDs and might play a role in IVD degeneration or regeneration. Furthermore, the hypertrophic induction medium did not induce hypertrophy but did induce prehypertrophy. In addition, normoxia seems to be more beneficial for prehypertrophic differentiation of NPCs than hypoxia. PTHrP and IHH did not induce cell proliferation and ECM production or counteracted apoptosis in canine and human NPCs and thus did not have an anabolic effect. Lastly, IHH induced calcifications and these calcifications occur independently from collagen type X expression. More *in vitro* studies are needed to further elucidate the role of PTHrP and IHH in healthy and degenerated IVDs and to determine if PTHrP or IHH could be useful for the development of regenerative treatments.

Keywords: intervertebral disc degeneration, nucleus pulposus, nucleus pulposus cells, PTHrP, IHH, PTHR1, Ptc, Smo, prehypertrophy, collagen type X, calcifications.

2. Introduction

The healthy vertebral column and intervertebral disc

The vertebral column consists of cervical, thoracic, lumbar, sacral, and coccygeal vertebrae, and forms a central canal which encloses and protects the spinal cord. The vertebrae are interconnected by an intervertebral disc (IVD) and all IVDs together make up approximately 15-20% of the length of the vertebral column depending on different factors such as species, age, and disease state (1,2). The main functions of the IVDs are absorbing biomechanical forces and providing movement, flexibility, and stability to the vertebral column (2).

Each healthy intervertebral disc consists of four parts: a central nucleus pulposus (NP), an outer annulus fibrosus (AF), a transition zone (TZ) between the AF and NP, and cartilaginous endplates (EPs) between the IVD and subchondral bone of the vertebral end plates at the caudal and cephalic ends of the disc (**Figure 1**) (2-4).

Nucleus Pulposus – The healthy NP is a centrally located, mucoid, translucent, bean-shaped structure, and is mainly composed of water (over 80%) (3). During development, the human nucleus is highly cellular, but after birth the cell number in the NP is reduced and in the adult NP, the cell density is very low (2). The main cell of the healthy NP is the notochordal cell (NC) which is characterized by cytoplasmic vesicles and relatively few mitochondria (3). NCs are large, vacuolated cells, mainly arranged in clusters, and produce a extracellular matrix (ECM) rich in proteoglycans like aggrecan that are trapped in a network of collagen type II and elastic fibers (2,3,5-8). The proteoglycan molecules consist of a protein backbone with negatively charged glycosaminoglycan (GAG) side chains like chondroitin sulfate and keratin sulfate (3). These negatively charged GAGs play an important role in maintaining the high intradiscal pressure of the healthy NP by osmotically attracting water into the NP (5). NCs have great regenerative potential and restorative capacity for other cells, such as chondrocyte-like cells (CLCs) (6), which are small, spherical and non-vacuolated NP-derived cells with little cytoplasm (7), and mesenchymal stromal (stem) cells (MSCs). In the NP during IVD degeneration, CLCs replace the NCs. These CLCs have regenerative potential but IVD degeneration can limit this regenerative potential of the CLCs. Therefore, the NCs play an important role and are an interesting focus for regenerative strategies (6).

Annulus Fibrosus – The healthy AF completely encircles the NP and is a dense network of multiple, organized, concentric fibrous lamellae and consists of 60% water (3). The lamellae consist of bundled fibrils, which mostly contain collagen type I strands held together by elastic fibers (3,5). The ventral part of the AF is 2 to 3 times thicker than the dorsal part, so during IVD degeneration, structural failure and IVD herniation are more common on the dorsal side. The outer layer of the AF contains elongated and fusiform fibrocyte-like cells, while the inner layer contains fibrocytes and spherical CLCs (2,3).

Transition Zone – Between the NP and the AF, the structure changes from a fibrous to a more cartilaginous/mucoid structure, also known as the TZ or innermost AF. In the TZ, CLCs are embedded in a loose fibrous matrix network, which contain predominantly collagen type II (2,3).

Cartilaginous endplates – The caudal and cephalic ends of the IVD are covered by cartilage, the endplate. The EPs contain chondrocytes mainly embedded in a collagen type II, highly hydrated ECM

(50-80%) and have three important functions (2,3). First, they serve as an interface between the NP and the bone of the vertebrae. Second, they serve as a biomechanical barrier that prevents the IVD from applying pressure directly to the bone, and third, they play an critical role in supplying the IVD with nutrients. Small molecules, like oxygen and glucose, reach the cells of the NP, TZ, and AF through diffusion and osmosis (2,3,9). In conclusion, the physiology of the IVD is mostly dependent on the quality of the ECM and therefore of the ability of its constituent cells to synthesize, remodel, and maintain a biochemically healthy matrix (3).

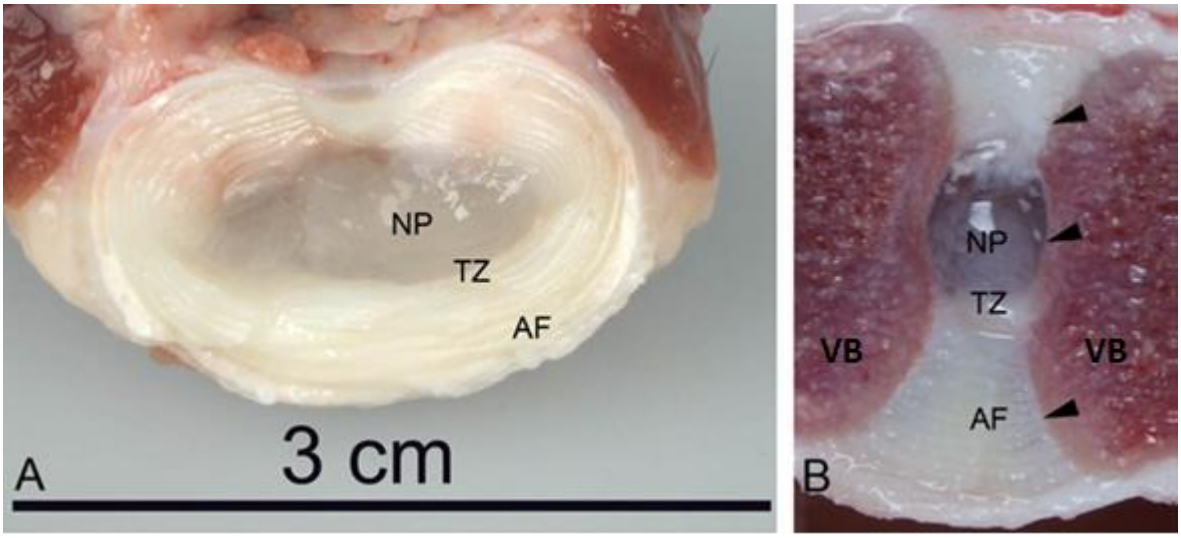

Figure 1. Transverse (A) and sagittal (B) sections through an canine intervertebral disc, showing the nucleus pulposus (NP), transition zone (TZ), annulus fibrosus (AF), cartilaginous endplates (arrow heads), and vertebral body (VB) (3).

The degenerated intervertebral disc

Degeneration of the IVD is a common phenomenon in humans and dogs, and can lead to different diseases such as disc herniation (2,3,10). IVD degeneration is considered the main cause of acute and chronic low back pain in humans, with a lifetime prevalence of over 70% in the global population. Also, it can lead to neurological clinical signs, and because the human IVD is more heavily innervated than the canine IVD, humans sometimes have symptoms of discomfort associated with IVD degeneration without actual herniation (5). In dogs, however, IVD degeneration is sometimes present without clinical signs of disease (11-13). Because IVD degeneration can cause (chronic) pain, physical disability, psychological distress, and a lower quality of life (14,15), it results in a serious socioeconomic burden with a total cost of $100 billion per year in the US (7).

Also dogs commonly suffer from back pain because of IVD degeneration. The dog is a unique species, because two subspecies can be distinguished based on their physical appearance, namely chondrodystrophic (CD) and non-chondrodystrophic (NCD) breeds (6,16,17). In CD breeds, replacement of NCs by CLCs start around 1 year of age, and IVD disease (IVDD) typically develops around 3-7 years of age. However, in NCD breeds, and especially in large-breed dogs, NCs remain the predominant cell type until middle or old age, and if an IVDD-related disease develops, it occurs around 6-8 years of age (6,16). Because dogs also commonly suffer from back pain, and IVD degeneration in dogs is very similar to IVD degeneration in humans, dogs are considered as a suitable animal model for human IVD degeneration (3,10).

During IVD degeneration, changes in the composition of the cells and the ECM of the NP, AF, TZ, and EPs occur (6) (**Figure 2**). Because the IVD is avascular and contain a low cell-density, the IVD cells are not able to adequately repair the ECM (3) so continuous damage occurs and therefore a vicious circle arises which will lead to IVD degeneration rather than healing. In other words, once the degenerative process starts, it is progressive (6). The early stage of IVD degeneration shows disorganization of the tissue structure, mainly by cellular changes within the NP and AF. In the NP, the large NC clusters are lost, resulting in smaller NC clusters or single NCs. IVD degeneration also involves a change in cellular phenotype from NCs to CLCs, and the glycosaminoglycan (GAG) and water content of the NP decreases (3,5,10,16). Because the cellular composition and the abnormal homeostasis of the ECM and ECM-regulating enzymes changes, the quality of the ECM deteriorates and this results in increasing numbers of clefts and cracks (3). AF degeneration is characterized by the disorganization of the lamellar fibers and the ingrowth of CLCs from the TZ (3,5). Due to the decreased GAG and water content in the NP, the NP is no longer able to maintain the high intradiscal pressure. Because of this, the AF is unable to provide normal movement and consequently, this leads to tensile forces that stress the AF and the endplate which may result in rupture or bulging of the AF (3,8). Also cross-links between the AF fibers are more common in degenerated than in healthy IVDs, and prevent lamellar movement in the AF which makes the AF stiffer (3). In the later stages of IVD degeneration, a marked loss of IVD space can be noted with new bone formation (3,5).

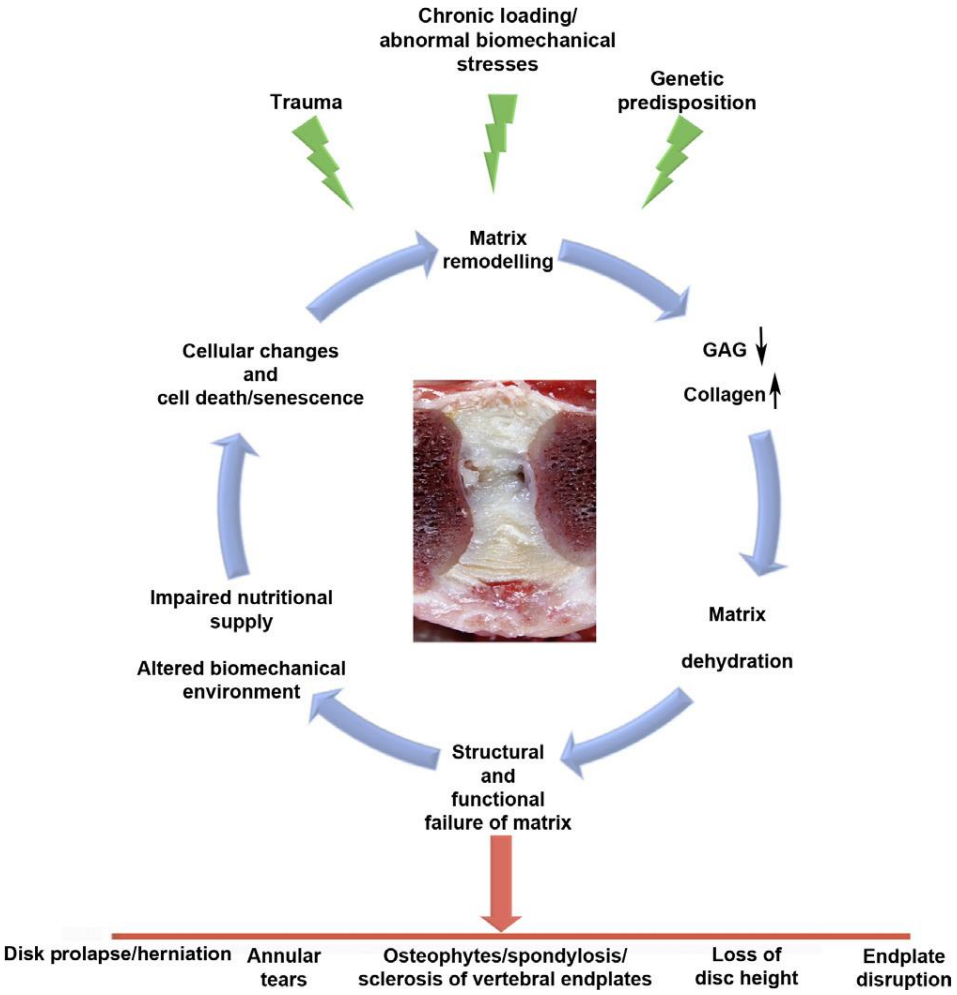

Figure 2. Schematic overview of the pathophysiology of intervertebral disc degeneration, illustrating the factors and the chain of events involved in the degenerative cascade partly based on human literature (3).

Current treatment options for intervertebral disc degeneration

Physiotherapy, medication, and surgery are current treatments for human and canine IVD degeneration, and are focused on relieving symptoms by reducing pain, and spinal cord and/or nerve decompression (16,18). However, these methods do not allow preservation of the IVD function for a longer period of time, and they are not curative. Therefore, within the field of regenerative medicine, the focus has been on strategies concentrating on biological repair of the degenerated IVD, e.g. using adult stem or progenitor cells, growth factors, and/or gene therapy (10). The aim of these therapies are to increase the cell numbers by stimulating proliferation of the resident cells by cell transplantation, and/or to stimulate matrix anabolism. Growth factors and peptides, like bone morphogenetic protein and Link N, have been shown to promote cell proliferation and/or matrix formation *in vitro* and/or *in vivo* in animal models with experimentally induced IVD degeneration. In addition, cell-based treatments using MSCs, articular chondrocytes, and CLCs derived from the NP have been tested (7). In spite of these therapies, further knowledge of the pathogenesis of IVD degeneration and the pathways involved is required. Some interesting pathways have not been studied yet, for instance the PTHrP-IHH pathway. Therefore it is important to determine the unexplored role of PTHrP and IHH in the healthy and degenerated IVD.

The role of Parathyroid hormone-related peptide and Indian Hedgehog during endochondral ossification

Parathyroid hormone-related peptide (PTHrP), the type 1 PTHrP receptor (PTHR1), Indian Hedgehog (IHH) and the receptors Patched (Ptc; IHH receptor) and Smoothened (Smo; transmembrane protein that activates downstream hedgehog-signaling; **Figure 3**) are signaling molecules, which are involved in the regulation of chondrocyte proliferation and differentiation, and form a PTHrP-IHH feedback loop in the growth plate (19,20).

During endochondral ossification, chondrocytes move through an orderly differentiation process, namely, from peri-articular proliferating chondrocytes to columnar proliferating chondrocytes to prehypertrophic chondrocytes to eventually hypertrophic chondrocytes. PTHrP is secreted by peri-articular proliferating chondrocytes, while its receptor, PTHR1, is mainly expressed in prehypertrophic chondrocytes (**Figure 4** and **Figure 5)** (21). PTHrP stimulates chondrocyte proliferation, inhibits apoptosis, and suppressed the maturation of prehypertrophic chondrocytes, thereby preventing further mineralization (21-23). Hypertrophic chondrocytes produce collagen type X. Proliferating chondrocytes secrete and maintain the cartilaginous ECM rich in collagen type II. Hypertrophic chondrocytes mineralize the surrounding ECM, secrete vascular endothelial growth factor to induce blood vessel formation, and finally undergo apoptosis. Then osteoblasts fill up the place left by hypertrophic chondrocytes and synthesize bone matrix, a process that results in new bone formation. The absence of PTHrP caused accelerated hypertrophic differentiation leading to premature mineralization of ECM and apoptosis. However, overexpression of PTHrP resulted in the opposite effect: delay of the terminal differentiation of chondrocytes, inhibition of apoptosis, and disruption of endochondral ossification (21).

PTHrP has a lot of similarities with Parathyroid hormone (PTH) in genetic sequence and structure. Additionally, PTHrP activates the same receptor (PTHR1) as PTH (24). In the NP and AF cells of the IVD, PTH increased collagen type II expression and decreased collagen type X expression (25). Presumably, PTHrP causes the same effect on expression level of collagen type II and collagen type X.

IHH is secreted by prehypertrophic and hypertrophic chondrocytes, and acts in conjunction with PTHrP to modulate endochondral ossification. IHH stimulates proliferating chondrocytes to produce PTHrP, which in turn accelerates the proliferation of peri-articular cells and prevents the onset of chondrocyte hypertrophy, keeping chondrocytes in a proliferating state (21,23). This negative feedback ensures orderly bone formation. However, IHH can also stimulate peri-articular chondrocyte proliferation and differentiation, and cause elongation of the columnar region independent of PTHrP (21,26). During endochondral bone formation, PTHrP-dependent IHH signaling inhibiting chondrocyte hypertrophy is dominant, thereby obscuring the promoting effect of PTHrP-independent IHH signaling (21).

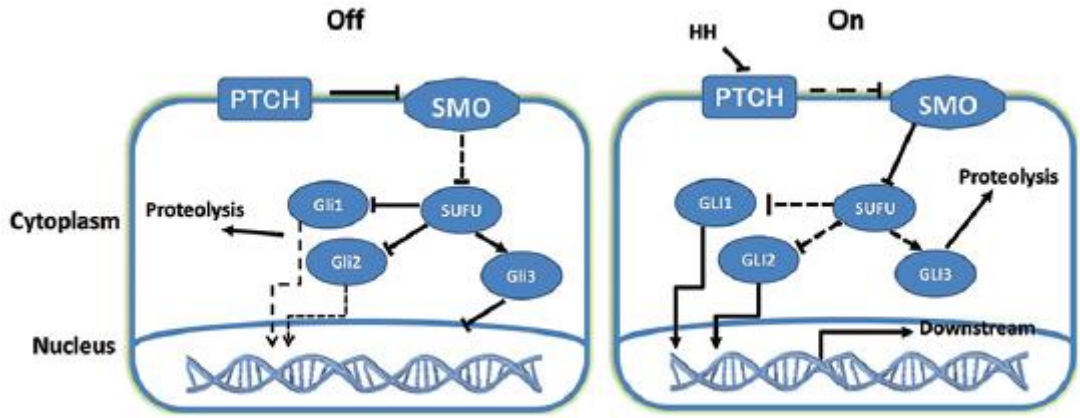

Figure 3. Indian Hedgehog (IHH) signaling pathway. When IHH is not present, Patched (Ptc) inhibits Smoothened (Smo) and represses the downstream IHH signaling pathway by suppressing GLI1 and GLI2 and promoting GLI3. When IHH is present, IHH binds to Ptc and releases Smo. The release of Smo activates the downstream IHH signaling pathway by promoting GLI1 and GLI2 expression (27).

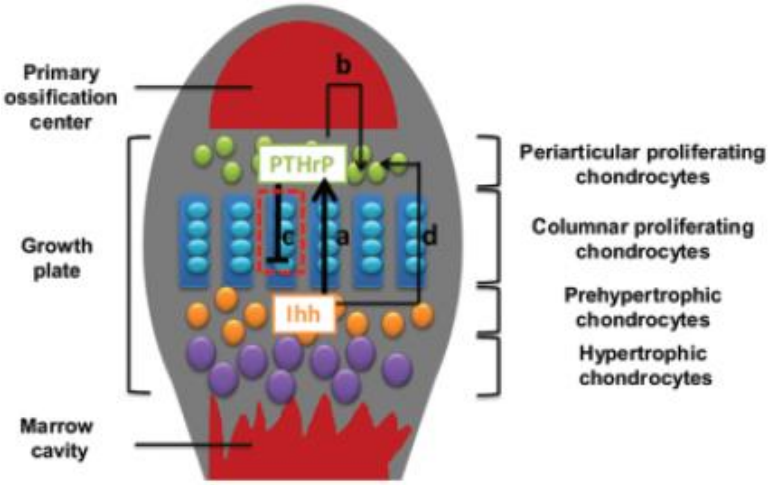

Figure 4. Parathyroid Hormone-related Peptide (PTHrP) - Indian Hedgehog (IHH) signaling pathway during endochondral ossification. **(a)** IHH (secreted by prehypertrophic chondrocytes) stimulates PTHrP production (synthesized by proliferating chondrocytes), **(b)** which in turn accelerates the proliferation of peri-articular chondrocytes, **(c)** and prevents chondrocyte hypertrophy. **(d)** In addition, IHH could stimulate peri-articular chondrocyte proliferation and differentiation independent of PTHrP (21,26).

During endochondral ossification, PTHrP and IHH are key players in a growth-restraining feedback loop in longitudinal bone growth, especially by determining the pace and synchrony of chondrocyte transition from proliferation into hypertrophic differentiation. IHH is partly responsible for the variation in final adult height, and PTHrP is one of the major predictors of growth rate width. According to *Tryfonidou et al. (2010)* there is a difference in the amount and ratio of PTHrP and IHH in the epiphyseal growth plate between small breed and large breed dogs. In large breed dogs, PTHrP levels are low but the IHH pathway is upregulated and more widely presented. However, in small-breed dogs there is proportionately more PTHrP than IHH. This difference between small breed and large breed dogs can be explained by the difference in growth plate morphology and growth rate. Growth plates of large breed dogs are wider and have larger proliferative and hypertrophic zones, probably because of the difference in the PTHrP-IHH feedback loop. IHH is relatively upregulated and PTHrP is relatively downregulated. As a result, the effects of IHH in the regulation of chondrocyte proliferation and hypertrophy can become more dominant during rapid growth rates (28).

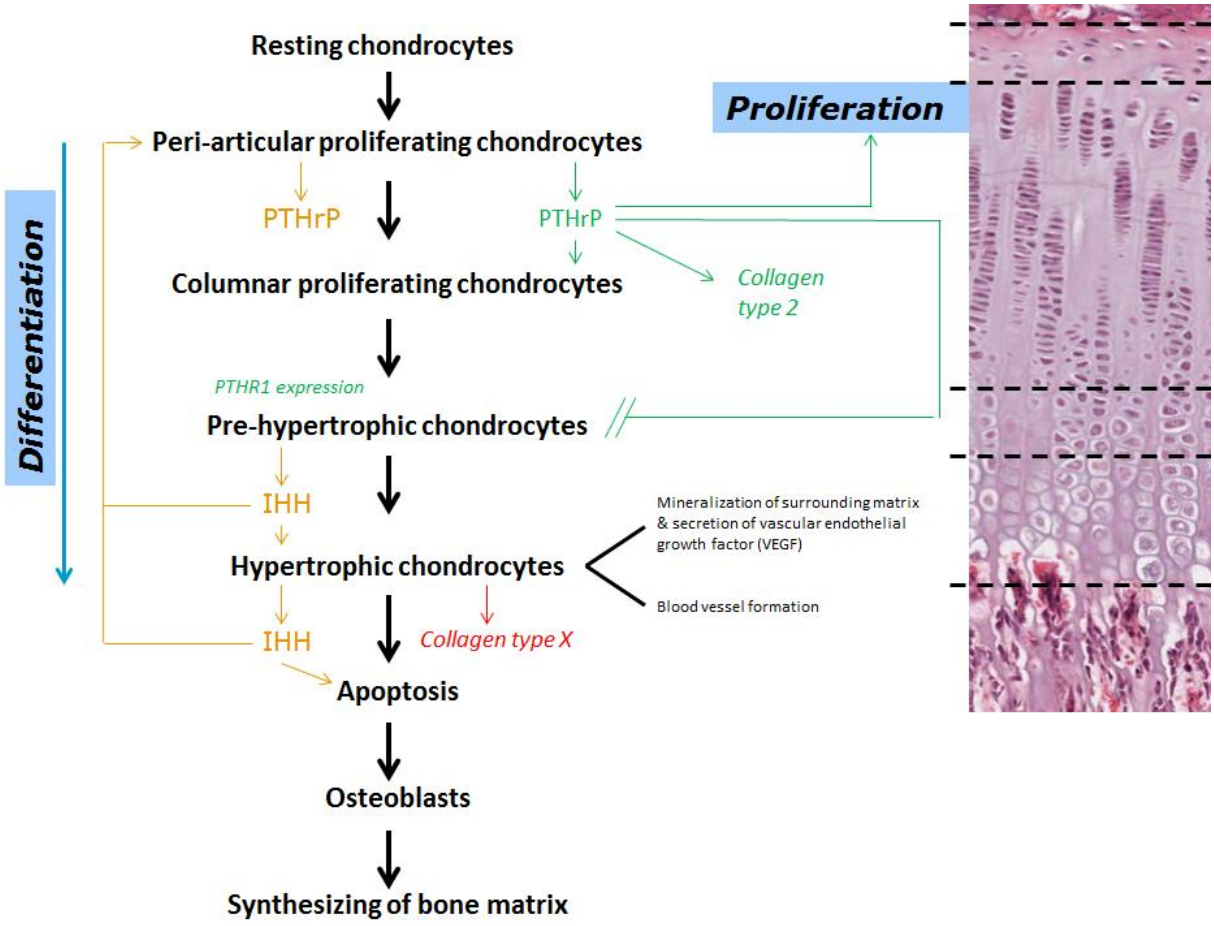

Figure 5. The Parathyroid hormone-related peptide (PTHrP) – Indian Hedgehog (IHH) signaling pathway during endochondral ossification in the growth plate.

The role of Parathyroid hormone-related peptide and Indian Hedgehog in articular cartilage

Also in articular cartilage, PTHrP and IHH play an important role. PTHrP could regulate articular chondrocytes and participate in the maintenance of articular cartilage as it did in growth plate cartilage (21,23). The PTHrP-producing cells, in both growth plate cartilage and articular cartilage, are derived from the same source, the chondroepiphysis, which is divided by the secondary ossification center into two distinct PTHrP-expressing subpopulations: the chondrocytes of the articular surface and peri-articular proliferating chondrocytes of the growth plate. However, PTHR1 is expressed in the underlying prehypertrophic chondrocytes (21).

Jiang et al. (2008) used co-culture models to evaluate the interaction of chondrocytes derived from three different layers of articular cartilage (surface, middle, and deep), and found that PTHrP, produced by the superficial or middle layer, is critical for the inhibition of mineralization in chondrocytes from the deep layer (23). This study shows *in vitro*, in healthy articular cartilage, that PTHrP secreted by surface layer chondrocytes inhibited the hypertrophic potential of deep layer chondrocytes so as to maintain the homeostasis of articular cartilage. However, the effect was not confirmed *in vivo*. More evidence was provide when knock-out mice with a deletion of PTHrP in midregion articular chondrocytes were used. The knock-out mice showed severe cartilage degeneration, indicating that PTHrP plays an important role in the physiological regulation of articular cartilage maintenance. Under pathological conditions, such as osteoarthritis (OA), chondrocyte hypertrophy can be reactivated in the repair process (21).

Hypertrophic differentiation is a process characterized by the induction of collagen type X (29). *Rutges et al. (2010)* suggested that the process of hypertrophic differentiation also occurs in and is part of the process of IVD degeneration, and that hypertrophic differentiation occurs with an accompanying increase in calcification. Calcification in advanced stages of IVD degeneration could be a final result of the ongoing hypertrophic differentiation (29). Expression of PTHrP in articular cartilage is 5.42-fold higher than that of osteophytic chondrocytes, which represents a prototype of cartilage repair tissue. It is likely that the decreased expression of PTHrP is insufficient to inhibit abnormal hypertrophy in repair tissue. Therefore, supplement of exogenous PTHrP to diseased cartilage, and perhaps to degenerated IVDs, could be of great significance (21).

Study aim

The overall aim of this study was to determine the expression and possible role of PTHrP and IHH in human degenerated IVDs. During this study, ***(1)*** the expression of PTHrP, IHH, and their receptors (PTHR1, Ptc and Smo) in human IVDs of different degeneration grades, and ***(2)*** the effect of PTHrP on degenerated canine and human CLCs, including the effect of PTHrP supplementation on IHH signaling in the NP, were defined.

3. Materials and methods

3.1. Determination of PTHrP and IHH protein expression in healthy and degenerated human NPCs

3.1.1. Human NP tissue sources

IVD tissue (Thompson grade I to V) was collected from 22 human (L3-L5) donors for PTHrP, PTHR1, IHH, Ptc, and Smo immunohistochemistry. The human samples were of various age (14-88 years) and gender (15 female, 10 male), and were divided into 5 stages according to the grading scheme of Thompson, based on gross morphology of midsagittal sections, ranging from a healthy IVD (grade I) to a severely degenerated IVD (grade V). Herniation and prolapse of the IVD is not included in this grading scheme (3). The number of human samples per grade were: 5 Thompson grade I, 4 Thompson grade II, 4 Thompson grade III, 5 Thompson grade IV, and 4 Thompson grade V (**Table 1**). These human IVDs were obtained during standard *post mortem* diagnostics, as approved by the scientific committee of the Pathology department (University Medical Centre Utrecht (UMCU)). Anonymous use of redundant tissue for research purpose is a standard treatment agreement with UMCU patients. The material was used in line with the code 'Proper Secondary Use of Human Tissue' as installed by the Federation of Biomedical Scientific Societies.

Donor	Level	Age (years)	Gender	Cause of death
Thompson grade I				
S07-53	L3-L5	17	M	Neuro trauma
S07-3	L3-L5	21	F	Cardiac failure
S07-47	L3-L5	14	F	Unknown
S07-218	L3-L5	14	M	Unknown
S07-130	L3-L5	18	F	Cardiomyopathy
Thompson grade II				
S07-280	L3-L5	63	M	Sepsis
S07-295	L3-L5	35	M	Gastric carcinoma
S07-171	L3-L5	50	F	Aorta rupture
S07-184	L3-L5	39	M	Rejection lung transplant
Thompson grade III				
S07-23	L3-L5	73	F	Cerebral infarction
S07-234	L3-L5	80	F	Pneumonia
S07-292	L3-L5	46	F	Lung transplantation
S07-137	L3-L5	59	F	Sepsis
Thompson grade IV				
S07-276	L3-L5	88	F	Cerebral bleeding
S07-304	L3-L5	73	F	Acute cardiac arrest
S07-312	L3-L5	84	M	Cardiac failure
S07-250	L3-L5	70	F	Cerebral tumor
S07-195	L3-L5	77	M	Myocardial infarction
Thompson grade V				
S06-251	L3-L5	62	F	Cerebral haemorrhage
S06-179	L3-L5	59	M	Hepatocellular carcinoma
S07-69	L3-L5	71	M	Myocardial infarction
S06-287	L3-L5	88	F	Gastro-intestinal bleeding

Table 1. Human intervertebral disc (IVD) donor characteristics. Male (M); Female (F).

3.1.2. PTHrP, PTHR1, IHH, Ptc and Smo protein expression in the NP of human IVDs

Histology

Sections of the human IVDs on Microscope KP plus slides ((KP-3056, Klinipath B.V.) were readily available for histology.

PTHrP, PTHR1, IHH, Ptc and Smo immunohistochemistry

Immunohistochemical staining for PTHrP, PTHR1, IHH, Ptc, and Smo was performed on human IVDs using the goat polyclonal IgG kit (sc-2053, Santa Cruz Biotechnology Inc.). The sections were deparaffinized through xylene (two times 5 min) and graded ethanol (96%, 80%, 70%, 60%; 5 min each), followed by one PBS (1.37 M NaCl, 27 mM KCl, 101 mM Na_2HPO_4 and 18 mM KH_2PO_4) + 0.1% Tween (PBST0.1%) rinse (5 min). Antigen retrieval was performed with citrate buffer (10 mM, pH 6, 0.05% Tween) for 30 min at 70 ^{o}C. After washing with PBST0.1% (two times 5 min), the sections were blocked with peroxidase for 5 min at RT, and washed in PBST0.1% (for two times 5 min) again. Thereafter, the sections were blocked with donkey serum for 30 min at RT, and the sections were incubated overnight at 4^{o}C with primary antibody PTHR1 (1:20 dilution, sc-12777, Santa Cruz Biotechnology Inc.), PTHrP (1:25 dilution, sc-9680, Santa Cruz Biotechnology Inc.), IHH (1:50 dilution, sc-1196, Santa Cruz Biotechnology Inc.), Ptc (1:50 dilution, sc-6149, Santa Cruz Biotechnology Inc.) or Smo (1:25 dilution, sc-6366, Santa Cruz Biotechnology Inc.). In control staining for PTHrP, PTHR1, and IHH, the primary antibody was omitted. For Ptc, patched blocking peptide (1:5 dilution, sc-6149 P, Santa Cruz Biotechnology Inc.) in serum block with Ptc antibody (1:50 dilution, sc-6149, Santa Cruz Biotechnology Inc.) was used, and for Smo, smoothened blocking peptide (1:5 dilution, sc-6366 P, Santa Cruz Biotechnology Inc.) in serum block with Smo antibody (1:25 dilution, sc-6366, Santa Cruz Biotechnology Inc.) was used. All these negative controls showed no positive staining. As a positive control, we used endothelial cells, osteoblasts, and osteoclasts, among others, because we knew that they expressed the protein that we were interested in (**Table 8**). The next day, sections were washed with PBST0.1% (two times 5 min) before the secondary antibody was applied for 30 min at RT. After incubating, the sections were washed with PBS (two times 5 min), then incubated with HRP-Streptavidin Complex for 30 min at RT, and washed with PBS (two times 5 min) again. After washing, the sections were incubated with the DAB peroxidase substrate solution (K3468, DAKO) for 1 min, then rinsed in running tap water for 15 min, and thereafter counterstained with Haematoxylin QS solution (H3404, Vector Laboratories Inc., Burlingame, CA, USA) for 1 min. Lastly, they were washed with tap water for 15 min, dehydrated with graded ethanol (70%, 80%, 95% and 100%) and xylene (two times 5 min), and mounted (Vectamount, H5000, Vector Laboratories Inc.).

3.2. Testing the effect of PTHrP and IHH on early degenerated NPCs

3.2.1. Canine NP tissue sources

NPCs from 6 canine CD donors of various age (2-6 years) and gender (1 female, 5 male) were readily available for this study (**Table 2**).

Donor	Breed	Age (years)	Gender	Thompson grade
C1	CD	6	M	2/3
C2	CD	6	M	2/3
C3	CD	5	M	2/3
C4	CD	2	M	2/3
C5	CD	2	M	2/3
C6	CD	5	F	2/3

Table 2. Canine nucleus pulposus (NP) tissue donor characteristics. Chondrodystrophic breed (CD); Male (M); Female (F).

3.2.2. Culture conditions

Canine NPCs ($1 \cdot 10^{-6}$, P0) were expanded in a T175 culture flask (660175 CELLSTAR Greiner Bio-one) in 20 mL expansion medium (hgDMEM+GlutaMAX+pyruvate (31966, Invitrogen), 10% Fetal Bovine Serum (FBS) (Gibco 16000-044, Life Technologies), 1% Penicillin/Streptomycin, 0.1 mM Ascorbic acid 2-phosphate (A8960, Sigma-Aldrich), 0.001 µM dexamethasone (AD1756, Sigma-Aldrich), 1 ng/mL bFGF (PHP105, AbD Serotec), and 5 µl/mL fungizone (15290-018, Invitrogen)), and incubated at 5% O_2, 5% CO_2, 37 °C (P1). The expansion medium was changed twice a week. After 14 days the NPCs reached 90% confluence in P1. The medium was removed from the T175 flask and the cells were rinsed with 10 mL Hanks HBBS (for two times) to remove the FBS. Subsequently, 4 mL trypsin was added in order to detached the cells from the bottom of the T175 flask, and incubated for 15 min at 37°C. After incubating, 10 mL hgDMEM + 10% FBS was added to inactivate the trypsin. The NPCs were collected in a 50 mL tube, and centrifuged for 5 min at RT (1500 RPM). After centrifuging, the medium was replaced with chondrogenic differentiation culture medium and NPCs were counted to be able to form micro-aggregates of 35,000 cells. The NPCs were plated in Ultra-low attachment 96-well plates with a cell-repellent surface (650970, CELLSTAR® Greiner Bio-one) in 50 µl chondrogenic differentiation culture medium (hgDMEM+GlutaMAX+pyruvate, 1% ITS+ premix (354352, Corning Life Sciences) , 0.04 mg/mL L-proline (P5607, Sigma-Aldrich) , 1% Penicillin/Streptomycin, 0.1 mM Ascorbic acid 2-phosphate, 5 µl/mL fungizone, and 1.25 mg/mL Bovine Serum Albumin (A9418, Sigma-Aldrich)). The 96-wells plates were centrifuged for 5 min to induce micro-aggregate formation, and incubated at 5% O_2, 5% CO_2, 37 °C (P2, day 0). The next day, the chondrogenic differentiation culture medium was replaced with chondrogenic differentiation culture medium for the negative control micro-aggregates, and the remaining micro-aggregates with 10^{-7} M PTHrP (pTH-related Protein (1-34)amide, H-9095, Bachem), 10^{-8} M PTHrP, 0.1 µg/mL IHH (1705-HH, R&D Systems), or 1 µg/mL IHH (day 1; **Figure 6**). The concentration of 10^{-8} M PTHrP was based on previous work of *F. Bach et al. (2014) (24)* and the concentration of 0.1 µg/mL IHH was based on a reference of the manufacturer (*A.M. Handorf et al. (2015)* (30)). Two higher concentrations of PTHrP (10^{-7} M) and IHH (1 µg/mL) were chosen if the initial concentrations would have been too low to induce effects. The micro-aggregates were cultured for 14 days at 5% O_2, 5% CO_2, 37 °C. Medium of the micro-aggregates was changed two times per week.

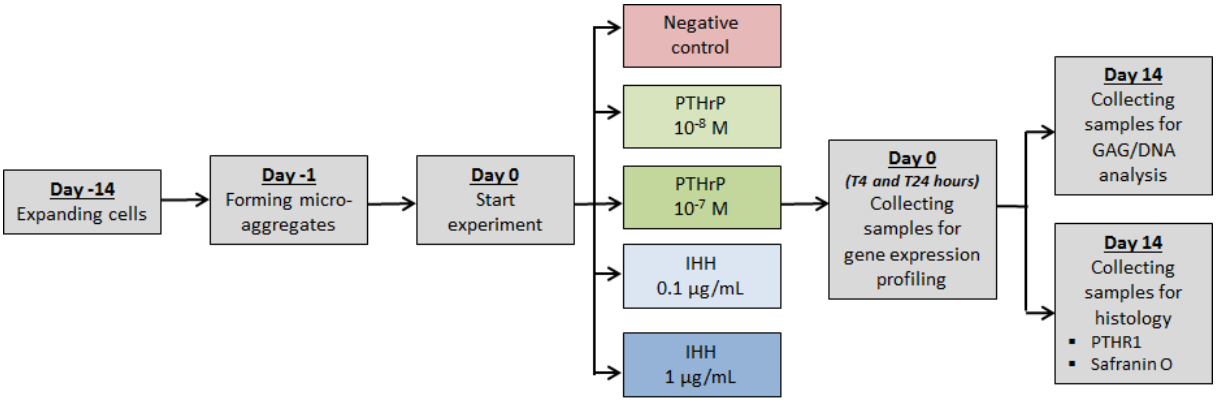

Figure 6. Time schedule and setup of the first *in vitro* micro-aggregate culture of canine nucleus pulposus cells (NPCs) (passage 0). On day -14, the NPCs were expanded (passage 1). The NPCs reached 90% confluence after 14 days (day -1), were plated in 96-wells plates, and centrifuged to induce micro-aggregate formation (passage 2). On day 0, there were five culture conditions created: the negative control which contained only chondrogenic differentiation culture medium, 10^{-8} M Parathyroid hormone-related peptide (PTHrP), 10^{-7} M PTHrP, 0.1 µg/mL Indian hedgehog (IHH), and 1 µg/mL IHH. After 4 and 24 hours, canine NPC micro-aggregates were collected and per donor pooled for gene expression profiling. On day 14, NPCs of the canine micro-aggregates were collected for histology to detect the Parathyroid hormone-related peptide receptor type 1 (PTHR1) and proteoglycans (Safranin O/Fast Green) expression, and NPCs and medium were collected for GAG/DNA analysis.

3.2.3. Cell proliferation and extracellular matrix production of the canine NPC micro-aggregates

DNA and GAG content

On day 14, NPCs and medium of the canine NPC micro-aggregates (**Table 2**) were collected and stored at -20 °C to determine DNA and GAG content. Before determining DNA and GAG content, papain digestion was performed to digest the canine NPC micro-aggregates. Samples were lyophilized for 30 min (Savant SpeedVac System AES 2010 Concentrator) and after lyophilizing, papain digestion solution (pH 6, 200 mM H_2NaPO_4*2 H_2O (21254, Boom B.V.), 10 mM EDTA (100944, Merck Millipore), 10 mM cysteine HCl (C7880, Sigma-Aldrich), and 10 mM papain (P3125, Sigma-Aldrich) was added to each NPC micro-aggregate, followed by overnight incubation at 60 °C. To measure the DNA content of the NPC micro-aggregates, the Qubit dsDNA High Sensitivity Assay Kit (Q32851, Invitrogen) was used according to the guidelines of the manufacturer. A dimethylmethylene blue (DMMB) assay was performed to determine the GAG content of the NPC micro-aggregates and the medium. The DMMB substance associates with negatively charged GAG side chains, after which a shift in the absorption maximum can be observed. A standard line was generated by stepwise dilution of chondroitin sulphate C (C4384-250 mg, Sigma-Aldrich). The absorbance (540 and 595 nm) was measured using a microplate reader (Model 3550, Bio-Rad) and the GAG content per sample was calculated according to the polynomic formula ($y=ax^2+bx+c$) obtained by the standard curve.

Histology

Sections of the canine NPC micro-aggregates (**Table 2**) on Microscope KP plus slides were readily available for histology.

Safranin O/Fast Green staining

Safranin O/Fast Green staining was performed to stain proteoglycans in canine NPC micro-aggregates (**Table 2**). The sections were deparaffinized as described previously, followed by one rinse with PBS for 5 min, one rinse with citrate for 15 min and washed with Milli Q for 5 min. After this, the sections were subjected to Weigert's haematoxylin (solution 1; 640495, solution 2; 640505, Klinipath B.V.) for 5 min and rinsed with running tap water for 10 min. Furthermore, sections were stained with 0.4% aqueous Fast Green (F7252, Sigma-Aldrich) for 4 minutes, rinsed in two changes of 1% Acetic Acid (5 min each; 76051830, Boom) and stained with 0.125% aqueous Safranin O (S8884, Sigma-Aldrich) for 5 min. Lastly, sections were dehydrated with 96% ethanol two times (3 min each), 100% ethanol (2 min) and xylene (two times 3 min) and mounted (Vectamount, H5000, Vector Laboratories).

Parathyroid hormone-related peptide receptor type 1 immunohistochemistry

Immunohistochemistry staining for PTHR1 was performed on canine NPC micro-aggregates (**Table 2**). The micro-aggregates were stained as described earlier, except that the sections were incubated with the DAB peroxidase substrate solution (K3468, DAKO) for 5 min instead of 1 min.

3.2.4. Gene expression of the canine NPC micro-aggregates

In order to determine the transcriptional effect of PTHrP or IHH supplementation on NPCs (**Table 2**), RNA isolation, cDNA synthesis, and Real-Time quantitative Polymerase Chain Reaction (RT-qPCR) analysis were performed.

RNA isolation

After 4 and 24 hours of treatment, canine NPC micro-aggregates per donor were pooled and collected for RNA isolation. Micro-aggregates were frozen in liquid nitrogen and crushed with pestles (P9951-901, Argos Technologies). After crushing, 350 µL buffer RLT + β-mercaptoethanol (74004, Qiagen) was added. To note, during the crushing procedure of the RNA isolation particular attention was required to avoid RNA degradation by active RNases, which were released during the lysis step. So, RNases were rapidly and thoroughly inactivated with RLT + β-mercaptoethanol to obtain high-quality RNA. After adding 350 µL buffer RLT + β-mercaptoethanol, the RNA was further lysed and homogenized by pipetting up and down. Thereafter, the samples were vortexed and frozen in liquid nitrogen. The samples were placed on ice and stored at -70 °C until use.

RNA was isolated by using the RNeasy Micro Kit (74004, Qiagen). First, the RNA samples were centrifuged at max speed for 5 min and in the meantime 70% ethanol was added to new vials. After centrifuging, the supernatant was transferred to the new vials with 70% ethanol, mixed and transferred to Microkit columns. The Microkit columns were centrifuged at max speed for 30 seconds and the flow through the filters of the columns were discarded. Thereafter, the Microkit columns were washed with 350 µL RW1 buffer (RNeasy Microkit), then centrifuged at max speed for 30 seconds ones more, and the flow through the filters of the columns were discarded. Thereafter, 80 µL DNase (RNAse free DNAse Set, 79254) was added on the membrane of the columns to ensure DNA removal, and incubated for 15 min. After incubating, 350 µL RW1 buffer was added and the columns were centrifuged at max speed for 30 seconds. Collection tubes were discarded and 500 µL RPE+ buffer was added. The columns were centrifuged at max speed for 30 seconds and after centrifuging the flow through the filters of the columns were discarded. Thereafter, 500 µL 80% ethanol was added and centrifuged at max speed for 2 min. The collection tubes were discarded and

the columns were centrifuged at max speed for 5 min with open lids. Further, 17 µL RNase free water was directly added on the membrane of the columns and incubated for 1 min. After incubating, the columns were centrifuged in 1,5 mL tubes at max speed for 1 min. The flow through the filters of the columns were transferred to the membrane of the columns, centrifuged at max speed for 1 min, and after centrifuge stored at -70 °C until use. The quality of the isolated RNA was tested with an Agilent 2100 Bioanalyzer and RNA Nanochip Kit (5067-1511, Agilent Technologies).

cDNA synthesis and RT-qPCR

cDNA was synthesized using the iScript cDNA Synthesis Kit (170-8891, Bio-Rad) according to the manufacturer's instructions. Primer sequences for RT-qPCR were obtained from previous work in a supplementary file. Four stable expressed reference genes (glyceraldehyde 4-phosphate dehydrogenase (GAPDH), hypoxanthine phosphoribosyltransferase (HPRT), Ribosomal Protein S19 (RPS19) and succinate dehydrogenase complex flavoprotein subunit A (SDHA)) where chosen to normalize for the target gene expression of ECM anabolism, ECM catabolism, proliferation, apoptotic markers, NP markers, PTHrP-IHH signaling, smad-signaling, and others (**Table 3**).

RT-qPCR was performed using the iQT SYBR Green Supermix Kit (Bio-Rad) and the CFX384 Touch Real-Time PCR Detection System (Bio-Rad). RT-qPCR was performed to assess the effects of PTHrP or IHH at gene expression levels on: **1)** ECM anabolism (aggrecan (*ACAN*), collagen type 1 (*COL1A1*), collagen type 2 (*COL2A1*), collagen type 10 (*COL10A1*)), **2)** ECM catabolism (a disintegrin and metalloproteinase with thrombospondin motifs 5 (*ADAMTS5*), matrix metalloproteinase 13 (*MMP13*), tissue inhibitor of metalloproteinase 1 (*TIMP1*)), **3)** proliferation (cyclin D1 (*CCND1*)), **4)** apoptotic markers (B-cell lymphoma 2-associated X (*BAX*), B-cell lymphoma 2 (*BCL-2*), caspase 3 (*CASP3*)), **5)** NP-specific markers (forkhead box F1 (*FOXF1*), keratin 8 (*KRT8*), keratin 18 (*KRT18*), keratin 19 (*KRT19*), T brachyury transcription factor (*T*)), **6)** PTHrP-IHH signaling (parathyroid hormone related-peptide (*PTHrP*), PTHrP receptor 1 (*PTHR1*), indian hedgehog (*IHH*), patched (*Ptc*), smoothened (*Smo*), Gli proteins (*GLI1, GLI 2, GLI3*)), **7)** Smad-signaling (inhibitor of DNA binding 1 (*ID1*), plasminogen activator inhibitor-1 (*PAI1*)), and **8)** others (runt-related transcription factor 2 (*RUNX2*), sex determining region Y-box 9 (*SOX9*), vascular endothelial growth factor (*VEGF*)). The Normfirst method was used to determine relative quantitative gene expression. For each target gene, the Cq-value of the test sample and the calibrator sample was normalized to the mean Cq-value of the reference genes ($\Delta Cq = Cq_{mean\ ref} - Cq_{target}$). Cq-values of the negative control micro-aggregates were used as calibrator. Thereafter, $E^{\Delta Cq}$-value was calculated for the test and calibrator sample whereby E indicates the amplification efficiency of the target or reference gene. Lastly, the $E^{\Delta Cq}$-value of the test sample was normalized to the $E^{\Delta Cq}$-value of the calibrator to calculate the $E^{\Delta\Delta Cq}$ ($E^{\Delta\Delta Cq} = E^{\Delta Cq\ test} - E^{\Delta Cq\ calibrator}$). For each target gene, the mean *n*-fold values and standard deviations in gene expression were calculated.

Genes	Forward sequence 5'→ 3'	Reverse sequence 5' → 3'	Amplicon size	Annealing temperature (°C)
Reference genes				
GAPDH	TGTCCCCACCCCCAATGTATC	CTCCGATGCCTGCTTCACTACCTT	100	58
HPRT	AGCTTGCTGGTGAAAAGGAC	TTATAGTCAAGGGCATATCC	104	58
RPS19	CCTTCCTCAAAAAGTCTGGG	GTTCTCATCGTAGGGAGCAAG	95	61
SDHA	GCCTTGGATCTCTTGATGGA	TTCTTGGCTCTTATGCGATG	92	61
Target genes				
ACAN	GGACACTCCTTGCAATTTGAG	GTCATTCCACTCTCCCTTCTC	111	61,5
ADAMTS5	CTACTGCACAGGGAAGAG	GAACCCATTCCACAAATGTC	149	61
BAX	CCTTTTGCTTCAGGGTTTCA	CTCAGCTTCTTGGTGGATGC	108	58
BCL-2	TGGAGAGVGTCAACCGGGAGATGT	AGGTGTGCAGATGCCGGTTCAGGT	87	62
CASP3	CGGACTTCTTGTATGCTTACTC	CACAAAGTGACTGGATGAACC	89	61
COL1A1	GTGTGTACAGAACGGCCTCA	TCGCAAATCACGTCATCG	109	61
COL2A1	GCAGCAAGAGCAAGGAC	TTCTGAGAGCCCTCGGT	151	63
COL10A1	CCAACACCAAGACACAG	CAGGAATACCTTGCTCTC	80	61
CCND1	GCCTCGAAGATGAAGGAGAC	CAGTTTGTTCACCAGGAGCA	117	58
FOXF1	GAGTTCGTCTTCTCCTTCAACAC	GCTTGATGTCTTGGTAGGTGAC	99	59.5
GLI1	TCAAGGCTCAGTACATGCTG	ATGGCTTCTCATTGGAGTGG	240	64
GLI2	CACGCTCTGGGAAATGAGG	CGGGCATCAGCAACATG	145	61
GLI3	CCAGCAGGAACAGCCAG	GAACTCCTTCTTCTCGCCG	190	64
ID1	CTCAACGGCGAGATCAG	GAGCACGGGTTCTTCTC	135	59.5
IHH	TCACCACTCAGAGGAGTCG	GTGCTCAGACTTGACGGAG	172	60
KRT8	CCTTAGGCGGGTCTCTCGTA	GGGAAGCTGGTGTCTGAGTC	149	63
KRT18	GGACAGCTCTGACTCCAGGT	AGCTTGGAGAACAGCCTGAG	97	60
KRT19	GCCCAGCTGAGCGATGTGC	TGCTCCAGCCGTGACTTGATGT	86	64
MMP13	CTGAGGAAGACTTCCAGCTT	TTGGACCACTTGAGAGTTCG	250	65
PAI1	AAACCTGGCGGACTTCTC	ACTGTGCCACTCTCATTCAC	98	61.5
PTC	CCTCCTCATATTTGGGGC	CACCTTCTTCTTTCGGGG	158	57
PTHrP	GTGTTCCTGCTGAGCTACTCG	ATGGGTGGTCGCCTTCTA	451	66.5
PTHR1	GACCACATCCTTTGCTGG	CAAACACCTCCCGTTCAC	217	51
RUNX2	AACGATCTGAGATTTGTGGGC	TGTGATAGGTGGCTACTTGGG	97	64
SMO	CTATGTGCTGTGCCAG	ATCACTCTGCCCAGTC	214	62
SOX9	CGCTCGCAGTACGACTACAC	GGGGTTCATGTAGGTGAAGG	105	63
T	AGACAGCCAGCAATCTG	TGGAGGGAAGTGAGAGG	115	53
TIMP1	GGCGTTATGAGATCAAGATGAC	ACCTGTGCAAGTATCCGC	120	66
VEGF	CTTTCTGCTCTCCTGGGTGC	GGTTTGTGCTCTCCTCCTGC	101	58

Table 3. Canine primer sequences, amplicon size, and annealing temperature of the reference and target genes that were used in Real-Time quantitative Polymerase Chain Reaction analysis (RT-qPCR).

3.3. Pilot: *In vitro* induction of hypertrophic differentiation of canine NPCs

A pilot study was carried out with hypertrophic differentiation induction medium to determine if this medium could induce hypertrophy in canine NPCs as is visible in the degenerative process of the IVDs.

3.3.1. Canine NP tissue sources

NPCs from 6 canine CD donors of various age (2-6 years) and gender (1 female, 5 male) were readily available for this study (**Table 4**). The NPCs of the 6 donors were pooled into one mix.

Donor	Breed	Age (years)	Gender	Thompson grade
NPC 1399617	Beagle	5	M	2/3
NPC 7140151	Beagle	6	M	2/3
NPC 7283679	Beagle	3	M	2/3
NPC 7207859	Beagle	5	M	2/3
NPC 7200013	Beagle	5	M	2/3
NPC 1208156	Beagle	2	M	2/3

Table 4. Canine nucleus pulposus (NP) tissue donor characteristics. Male (M); Female (F).

3.3.2. Culture conditions

The NPCs were generated from the canine NP tissue mix mentioned in **Table 4.** The canine NPCs were expanded as described earlier. After three days, NPCs reached 90% confluence in P1, and NPC micro-aggregates were formed as described earlier. The 96-wells plates were incubated at normoxic (21% O_2, 5% CO_2, 37 °C) or hypoxic conditions (5% O_2, 5% CO_2, 37 °C) (day 0). The next day, the chondrogenic differentiation culture medium of all the micro-aggregates was replaced with chondrogenic differentiation culture medium with TGF-β_1 (hgDMEM+GlutaMAX+pyruvate, 1% ITS+ premix, 0.04 mg/mL L-proline, 1% Penicillin/Streptomycin, 0.5 µL/mL TGF-β_1, 10 µL/mL BSA, 5 µL/mL Fungizone, and 5 µL/mL ASAP) to induce chondrogenic predifferentiation. The first condition (control) contained micro-aggregates (*n*=8) that were cultured for 28 days in chondrogenic differentiation culture medium with TGF-β_1 at 37 ^{o}C, 5% CO_2 and 21% O_2 (normoxic; 4 micro-aggregates (C-NX)) or 5% O_2 (hypoxic; other 4 micro-aggregates (C-HX)). In the second condition, micro-aggregates (*n*=8) were cultured in chondrogenic differentiation culture medium with TGF-β_1 for 7 days, and thereafter cultured in hypertrophic differentiation medium for 21 days at 37 ^{o}C, 5% CO_2 and 21% O_2 (normoxic; 4 micro-aggregates (C7H21-NX)) or 5% O_2(hypoxic; other 4 micro-aggregates (C7H21-HX)) for the entire culture period of 28 days (**Figure 7**). The hypertrophic differentiation medium consisted of hgDMEM+GlutaMAX+pyruvate, 1% ITS+ premix, 0.04 mg/mL L-proline, 1% Penicillin/Streptomycin, 10^{-9} M Dexamethason, 5 µL/mL β-glycerophosphate, 5 µL/mL ASAP, and 3.37 µL/mL 3,3',5-triiodo-L-thyronine (T3, Sigma), and this composition of the hypertrophic differentiation medium was based on previous work of *D. Gawlitta et al. (2012)* (31). The last condition contained micro-aggregates (*n*=8) that were cultured in chondrogenic differentiation culture medium with TGF-β_1 for 14 days, and thereafter cultured in hypertrophic differentiation medium for 14 days at 37 ^{o}C, 5% CO_2 and 21% O_2 (normoxic; 4 micro-aggregates (C14H14-NX)) or 5% O_2 (hypoxic; other 4 micro-aggregates (C14H14-HX)) for the entire culture period of 28 days. Medium of the micro-aggregates was changed two times per week. Taken together, 6

different experimental conditions were imposed on the micro-aggregates, which will be referred to as C-NX, C-HX, C14H14-NX, C14H14-HX, C7H21-NX, and C7H21-HX.

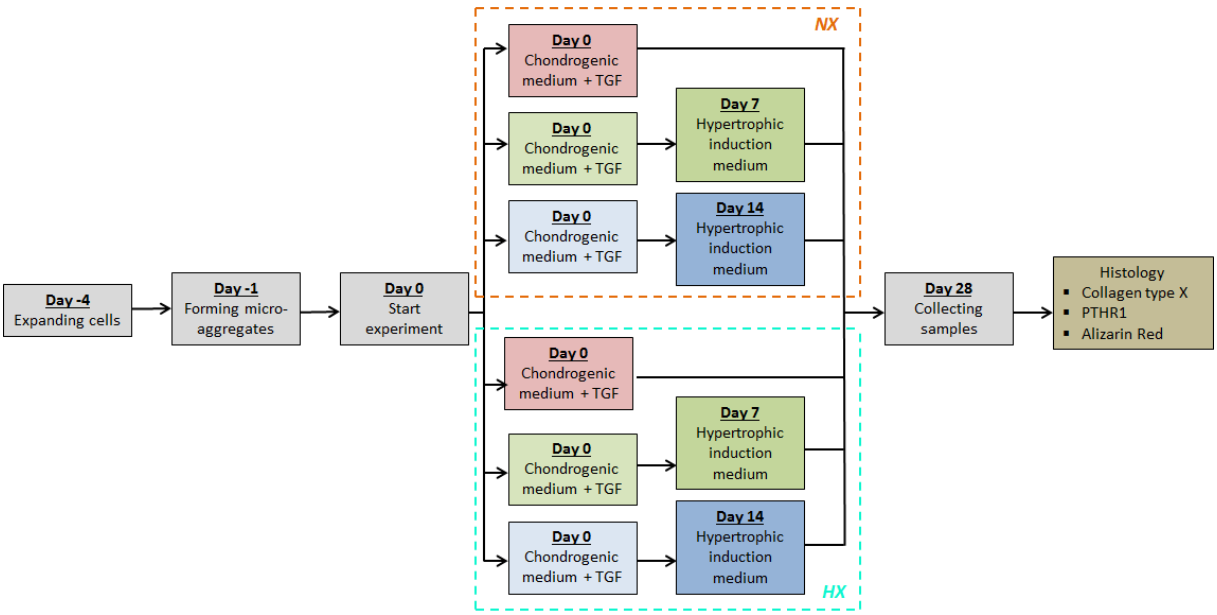

Figure 7. Time schedule and setup of the second *in vitro* micro-aggregate culture of canine nucleus pulposus cells (NPCs) (pilot study). In the first group (red), canine NPC micro-aggregates were cultured for 28 days in chondrogenic differentiation culture medium with TGF-β_1. In the second group (green), canine NPC micro-aggregates were cultured in chondrogenic differentiation culture medium with TGF-β_1 for 7 days, and thereafter cultured in hypertrophic induction medium for 21 days. In the third group (blue), canine NPC micro-aggregates were cultured in chondrogenic differentiation culture medium with TGF-β_1 for 14 days, and thereafter cultured in hypertrophic induction medium for 14 days. This experiment was generated under normoxic (21% O_2) conditions (NX) and hypoxic (5% O_2) conditions (HX). On day 28, NPCs of the canine micro-aggregates were collected for histology to detect the Parathyroid hormone-related peptide receptor type 1 (PTHR1) protein expression, collagen type X protein expression, and calcium (Alizarin Red).

3.3.3. Hypertrophic cell differentiation and extracellular matrix production of the canine NPC micro-aggregates.

Histology

To collect the canine NPC micro-aggregates (**Table 4**), the culture medium was removed and two micro-aggregates of the same condition were placed together in one well on day 28. Thereafter, the canine NPC micro-aggregates were fixed in 4% neutral buffered formaldehyde (4406-0240, Klinipath B.V.) containing 1% eosin (115935, Merck Milipore) for 24 hours at RT. Eosin was added to enable the detection of the micro-aggregates during the cutting process. The next day, the canine NPC micro-aggregates were embedded in 2.4% alginate (A2033, Sigma-Aldrich). The samples were dehydrated according to the protocol of the pathology department at Utrecht University, and embedded in paraffin. After embedding, 5-µm sections were fixed on Microscope KP plus slides.

Collagen type X immunohistochemistry

Immunohistochemical straining for collagen type X was performed on canine NPC micro-aggregates (**Table 4**) as marker for hypertrophic differentiation (29,32). The sections were deparaffinized as described previously, followed by one PBS and one PBST0.1% rinse (two times 5 min each). Antigen retrieval was performed with 0.1% Pepsin (P7000, Sigma) in 0.02 M HCl (100317, Merck) for 20 min

at 37 ^{o}C. After 20 min, the slides were washed with PBST0.1% (two times 5 min), and another antigen retrieval was performed with 10 mg/mL Hyaluronidase (H3506, Sigma-Aldrich) in PBS for 30 min at 37 ^{o}C. After washing with PBST0.1% (two times 5 min), the sections were blocked with Dual endogenous enzyme block (S2003, DAKO) for 5 min at RT. Thereafter, the sections were rinsed with PBS for one time and incubated afterwards with PBS for 5 min at RT. Normal goat serum (1:10 dilution) was diluted in PBST0.1% and incubated for 30 min at RT. Thereafter, the sections were incubated overnight at 4 ^{o}C with primary antibody collagen type X (1:50 dilution; 2031501005, Quartett) in 5% BSA (A3059, Sigma-Aldrich) in PBS. In control staining, the primary antibody was substituted with normal mouse IgG_1 (1:20000 dilution; 3877, Santa Cruz Biotechnology). This negative control showed no positive staining. The next day, sections were washed with PBST0.1% (two times 5 min) before the secondary antibody (EnVision + System-HRP Anti-Mouse, K4001, DAKO) was applied for 30 min at RT. After washing with PBS (two times 5 min), the sections were incubated with DAB peroxidase substrate solution (K3468, DAKO) for 1 min at RT and rinsed with MQ briefly. Thereafter, the sections were counterstained with hematoxylin QS solution (H3404, Vector Laboratories Inc.) for 20 seconds and rinsed in running tap water for 10 min. Lastly, the sections were dehydrated with graded ethanol (70%, 80%, 95%, and 100%) and xylene (two times 5 min), and mounted (Vectamount, H5000, Vector Laboratories Inc.).

Parathyroid hormone-related peptide receptor type 1 immunohistochemistry

Immunohistochemical staining for PTHR1 was performed on canine NPC micro-aggregates (**Table 4**) as marker of pre- and early hypertrophic differentiation (33,34). The micro-aggregates were stained as described earlier, except that the sections were incubated with the DAB peroxidase substrate solution (K3468, DAKO) for 5 min instead of 1 min.

Alizarin Red immunohistochemistry

Alizarin Red immunohistochemistry was performed to identify calcium, thus to detect calcification which occurs during hypertrophic differentiation (29), in canine NPC micro-aggregates (**Table 4**). The sections were deparaffinized as described previously, followed by one PBS rinse (5 min). The sections were incubated with 2% Alizarin Red Solution (pH 4.15; Sigma) for 45 min at RT, and washed with PBS (two times 5 min). Thereafter, the sections were counterstained (1 min), rinsed, dehydrated, and mounted as described earlier.

3.4. Testing the effect of PTHrP and IHH on hypertropically differentiated canine and human NPCs

3.4.1. Canine and human NP tissue sources

NPCs from 6 canine (**Table 5**) and 6 human donors (**Table 6**) were readily available for this study.

Canine donor	Age (years)	Gender	Passage
C1	6	M	P1
C2	6	M	P1
C3	5	M	P1
C4	2	M	P1
C5	2	M	P1
C6	5	F	P1

Table 5. Canine nucleus pulposus (NP) tissue donor characteristics. Male (M); Female (F)

Human donor	Age (years)	Gender	Passage
H1	63	F	P3
H2	72	M	P2
H3	44	M	P3
H4	47	M	P3
H5	56	M	P2
H6	50	M	P2

Table 6. Human nucleus pulposus (NP) tissue donor characteristics. Male (M); Female (F)

3.4.2. Culture conditions

NPCs were generated from the canine and human NP tissue mentioned in **Table 5** and **Table 6**. The canine and human NPCs were expanded as described earlier. After 3 days, NPCs reached 90% confluence, and NPC micro-aggregates were formed as described earlier except that most of the micro-aggregates (*n*=6 canine per culture condition and *n*=6 human per culture condition) were incubated in normoxic conditions (21% O_2, 5% CO_2, 37 °C) and only some micro-aggregates (*n*=3 canine and *n*=3 human per culture condition) were incubated in hypoxic conditions (5% O_2, 5% CO_2, 37 °C) on day 0 (**Figure 8**). In this culture experiment, 6 canine and 6 human NPC micro-aggregates per culture condition (all separated) were used for histology, while for RT-qPCR the canine and human NPC micro-aggregates per culture condition were pooled due to volume limitations of the micro-aggregates. For GAG/DNA analysis, 6 canine and 6 human NPC micro-aggregates per culture condition in duplo were used. The canine and human micro-aggregates were cultured for 49 days, and medium was changed three times a week. The first condition (control) contained micro-aggregates that were cultured for 49 days in chondrogenic differentiation culture medium supplemented with TGF-β_1 at 37 °C, 5% CO_2 and 21% O_2. In the second condition, micro-aggregates were cultured in chondrogenic differentiation culture medium supplemented with TGF-β_1 for 7 days, and thereafter cultured in hypertrophic induction medium for 42 days at 37 °C, 5% CO_2 and 21% O_2. In the third condition, micro-aggregates were cultured in chondrogenic differentiation culture medium supplemented with TGF- β_1 for 7 days, and thereafter cultured in hypertrophic induction medium for 42 days at 37 °C, 5% CO_2 and 21% O_2. In addition, from day 28 until day 49 the micro-aggregates were treated with 10^{-8} M PTHrP. The same applies to the fourth, fifth, and sixth condition except that the micro-aggregates were treated with 10^{-7} M PTHrP, or 0.1 µg/mL IHH, or 1 µg/mL IHH from day 28 until day 49. Besides all these micro-aggregates that were cultured in normoxic

conditions, 3 canine and 3 human NPC micro-aggregates per culture condition were cultured in hypoxic conditions (37 °C, 5% CO_2 and 5% O_2). The micro-aggregates that were cultured in hypoxic conditions were treated with chondrogenic differentiation culture medium supplemented with TGF-β_1 for 49 days, or with chondrogenic differentiation culture medium supplemented with TGF-β_1 for 7 days, and thereafter in hypertrophic induction medium for 42 days. The composition of the hypertrophic induction medium was based on previous work as described in part 3.3.1. Taken together, 8 different experimental conditions were imposed on the micro-aggregates per donor.

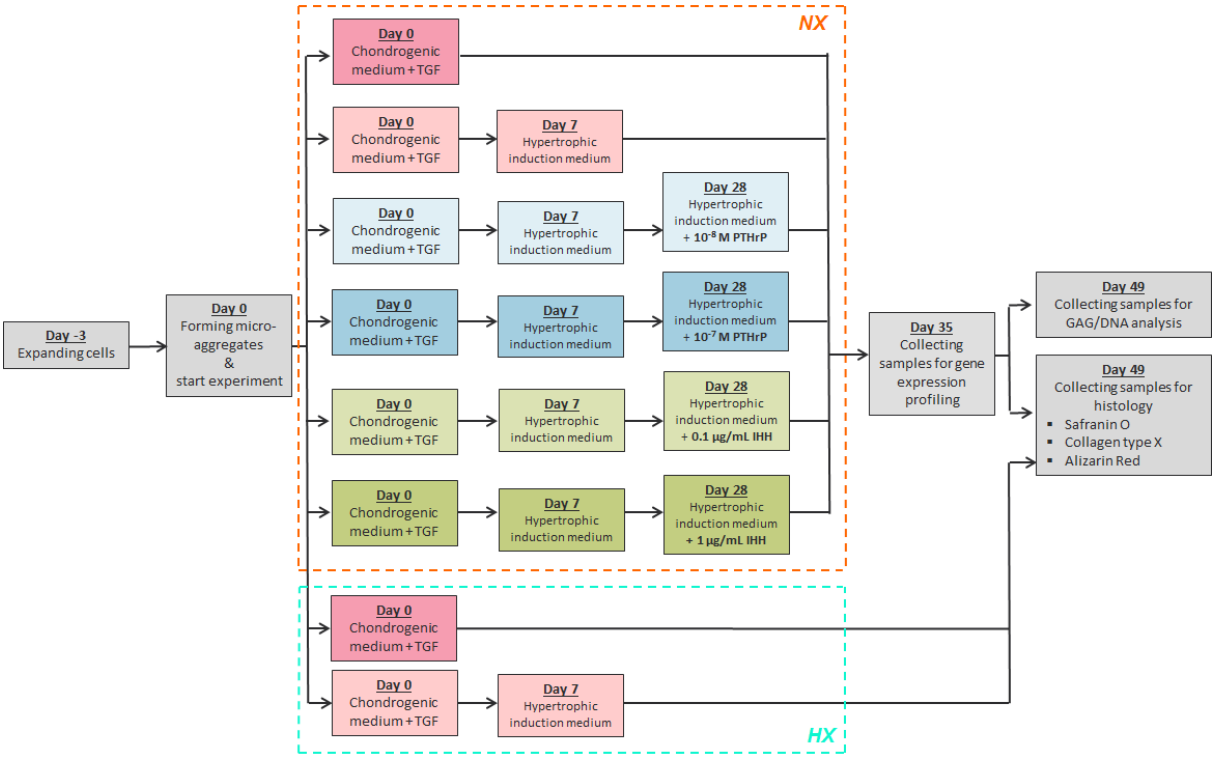

Figure 8. Time schedule and setup of the third *in vitro* micro-aggregate culture of canine nucleus pulposus cells (NPCs). In the first group (pink), canine and human NPC micro-aggregates were cultured for 7 days in chondrogenic differentiation culture medium supplemented with TGF-β_1. In the second group (light pink), canine and human NPC micro-aggregates were cultured in chondrogenic differentiation culture medium supplemented with TGF-β_1 for 7 days, and thereafter cultured in hypertrophic induction medium for 42 days. In the third group (light blue), canine and human NPC micro-aggregates were cultured in chondrogenic differentiation culture medium supplemented with TGF-β_1 for 7 days, and thereafter cultured in hypertrophic induction medium for 42 days. From day 28 until day 49, 10^{-8} M Parathyroid hormone-related peptide (PTHrP) was added to the hypertrophic induction medium. In the fourth (blue), fifth (light green), and sixth (green) group, the canine and human NPC micro-aggregates were cultured in the same medium, except that 10^{-7} M PTHrP, 0.1 µg/mL Indian Hedgehog (IHH), or 1 µg/mL IHH was added from day 28 until day 49. This experiment was mainly generated under normoxic (21% O_2) conditions (NX), but also under hypoxic (5% O_2) conditions (HX). On day 35, canine and human NPC micro-aggregates were collected for gene expression profiling. On day 49, NPCs and medium of the canine and human micro-aggregates were collected for GAG/DNA analysis and only NPCs for histology to detect the collagen type X protein, and to detect proteoglycans (Safranin O/Fast Green) and calcium (Alizarin Red).

3.4.3. Hypertrophic cell differentiation and extracellular matrix production of the canine and human NPC micro-aggregates

DNA and GAG content

On day 49, NPCs and medium of the canine and human NPC micro-aggregates (*n*=6 in duplo per culture condition; **Table 5** and **Table 6**) were collected to measure DNA and GAG content. DNA analysis and DMMB assay were performed as described in part 3.2.3.

Histology

To collect the canine and human NPC micro-aggregates (**Table 5** and **Table 6**), the culture medium was removed and two micro-aggregates of the same condition were placed together in one well on day 49. The fixation and embedding process was performed as described in part 3.3.3.

Safranin O/Fast Green immunohistochemistry

Safranin O/Fast Green immunohistochemistry was performed to stain proteoglycans in the canine and human NPC micro-aggregates (**Table 5** and **Table 6**) as described in part 3.2.3.

Collagen type X immunohistochemistry

Immunohistochemical staining for collagen type X was performed as described in part 3.3.3. on canine and human NPC micro-aggregates (**Table 5** and **Table 6**).

Alizarin Red immunohistochemistry

Alizarin Red immunohistochemistry was performed as described in part 3.3.3. on canine and human NPC micro-aggregates (**Table 5** and **Table 6**).

3.4.4. Gene expression of the canine and human NPC micro-aggregates

In order to determine the transcriptional effect of PTHrP and IHH supplementation on NPCs (**Table 5** and **Table 6**), RNA isolation, cDNA synthesis, and RT-qPCR analysis were performed.

RNA isolation

On day 35, canine and human NPC micro-aggregates (*n*=6 in duplo per culture condition) were collected for RNA isolation. RNA isolation was performed as described in part 3.2.4.

cDNA synthesis and RT-qPCR

cDNA synthesizes and RT-qPCR was performed as described in part 3.2.4. with the canine primers presented in **Table 3** and the human primers presented in **Table 4**. The same four stable expressed reference genes described in part 3.2.4. were chosen to normalize for the canine target gene expression, and four stable expressed reference genes (β-2-microglobulin (B2M), hypoxanthine phosphoribosyltransferase (HPRT), succinate dehydrogenase complex flavoprotein subunit A (SDHA), and TATA-box binding protein (TBP)) where chosen to normalize for the human target gene expression. Relative quantitative gene expression was determined by the Normfirst method. A description of this method is given in part 3.2.4. and the $E^{\Delta Cq}$-value of the test sample was normalized to the $E^{\Delta Cq}$-value of the calibrator to calculate the $E^{\Delta\Delta Cq}$ ($E^{\Delta\Delta Cq} = E^{\Delta Cq\ test} – E^{\Delta Cq\ calibrator}$). For each target gene, the mean *n*-fold values and standard deviations in gene expression were calculated.

Genes	Forward sequence 5'→ 3'	Reverse sequence 5' → 3'	Amplicon size	Annealing temperature (°C)
Reference genes				
B2M	CTTTGTCACAGCCCAAGATAG	CAATCCAAATGCGGCATCTTC	83	58
HPRT	AGCTTGCTGGTGAAAAGGAC	TTATAGTCAAGGGCATATCC	104	58
SDHA	GCCTTGGATCTCTTGATGGA	TTCTTGGCTCTTATGCGATG	92	61
TBP	TGCACAGGAGCCAAGAGTGAA	CACATCACAGCTCCCCACCA	132	63.5
Target genes				
ACAN	CAACTACCCGGCCATCC	GATGGCTCTGTAATGGAACAC	160	63.5
ADAMTS5	GCCAGCGGATGTGCAAGC	ACACTTCCCCCGGACGCAGA	-	62.5
BAX	GGACGAACTGGACAGTAACATGG	GCAAAGTAGAAAAGGGCGACAAC	-	58-64
BCL-2	ATCGCCCTGTGGATGACTGAG	CAGCCAGGAGAAATCAAACAGAGG	-	64
CASP3	CAGTGGAGGCCGACTTCTTG	TGGCACAAAGCGACTGGAT	-	55.5-59
COL1A1	TCCAACGAGATCGAGATCC	AAGCCGAATTCCTGGTCT	191	58-64
COL2A1	AGGGCCAGGATGTCCGGCA	GGGTCCCAGGTTCTCCATCT	195	62-63.5
COL10A1	CACTACCCAACACCAAGACA	CTGGTTTCCCTACAGCTGAT		
CCND1	AGCTCCTGTGCTGCGAAGTGGAAAC	AGTGTTCAATGAAATCGTGCGGGGT		65
FOXF1	ACCAGAACAGCCACAACG	AAAGAGAAGACAAACTCCTTTCGG	99	59.5
GLI2	AAGCCTTCTCCAACGCCT	GGTCTGTGTATCTCTTGGTGC	107	56.5-57
GLI3	CCTGTACCAATTGATGCCAG	GGAAGTCATATGCAATGGAGG	80	58.5
ID1	CTCTACGACATGAACGGCTGT	TGCTCACCTTGCGGTTCTG		62-66
IHH	GCCATTCTGAGGTATGACATTCCT	AACACAGAACTCTGCCCACAG	87	65-66
KRT8	GGATCTCCGCCTGGTTC	GACACCTTGTAGGACTTCTGGGTCA	92	63
KRT18	CGGGCATTGTCCACAGTATT	GGGAGCACTTGGAGAAGAAG	108	65
KRT19	CTTCCGAACCAAGTTTGAGAC	AGCGTACTGATTTCCTCCTC	183	64
MMP13	TCCCAGGAATTGGTGATAAAGTAGA	CTGGCATGACGCGAACAATA	-	64
PAI1	GCTGGTGAATGCCCTCTAC	GGCAGCCTGGTCATGTTG	-	64-65.5
PTC	CCCAAGCAAATGTACGAGCAC	TGCGACACTCTGATGAACCAC	132	57.7
PTHrP	CTCTGCCTGGTTAGACTCTG	TCAATGCCTCCGTGAATCG	102	65
PTHR1	CCATACACCGAGGTCTCAG	GATTTCTTGATCTCAGCTTGTACC	136	59
RUNX2	ACTGCTTGCAGCCTTAAAT	GTAACCCGTTGAACCCCATT	-	60
SMO	AGGCTGCACGAATGAGGTG	ACGTCCTCGTACCAGCTCTT	102	53
SOX9	CCCAACGCCATCTTCAAGG	CTGCTCAGCTCGCCGATGT	-	65.5
TIMP1	CTTCTGGCATCCTGTTGTTG	GGTATAAGGTGGTCTGGTTG	-	56-64
VEGF	TTGTACAAGATCCGCAGACG	GTCACATCTGCAAGTACGTTCG	101	62

Table 7. Human primer sequences, amplicon size, and annealing temperature of the reference and target genest hat were used in Real-Time quantitative Polymerase Chain Reaction analysis (RT-qPCR).

3.5. Statistical analysis

All data were statistically analyzed using SPSS Statistics 24 software (IBM). First, the data were examined for normal distribution using a Shapiro Wilks test. Non-normally distributed data were subjected to the Kruskal Wallis and Mann-Whitney U test, whereas general linear regression models based on ANOVAs were used for normally distributed data. All tests were followed by a Benjamini & Hochberg False Discovery Rate *post-hoc* test for multiple comparisons. A p-value<0.05 was considered significant. Biological significance between conditions was reached with at least a two times difference in value.

4. Results

4.1. Immunohistochemical evaluation of PTHrP, PTHR1, IHH, Ptc and Smo in human NP tissue of different degeneration grades

To study the expression patterns of the corresponding proteins, immunohistochemistry on human IVDs with different degeneration grades (Thompson grade I to V) was performed (**Figure 9**). The mean ratio of PTHrP positive cells significantly decreased from Thompson grade I to II (p<0.05; **Figure 10d**). However, the mean ratio of PTHrP positive cells significantly increased from Thompson grade II to IV, and from II to V (p<0.05). Also, PTHrP protein expression significantly increased from Thompson grade III to IV, and from III to V (p<0.05). The mean ratio of PTHR1 positive cells significantly decreased from Thompson grade I to III and I to V (p<0.05;**Figure 10e**). The mean ratio of IHH positive cells significantly decreased from Thompson grade I to II and I to III (p<0.05; **Figure 10a**). However, the mean ratio of IHH positive cells significantly increased from Thompson grade II to V and III to V (p<0.05). The mean ratio of Ptc positive cells significantly decreased from Thompson grade I to II and from I to III (p<0.01; **Figure 10b**). Also, Ptc protein expression significantly decreased from Thompson grade I to V (p<0.05). However, the mean ratio of Ptc positive cells significantly increased from Thompson grade II to IV and from III to IV (p<0.05). For the protein Smo, there were no significant difference between the different Thompson grades (**Figure 10c**).

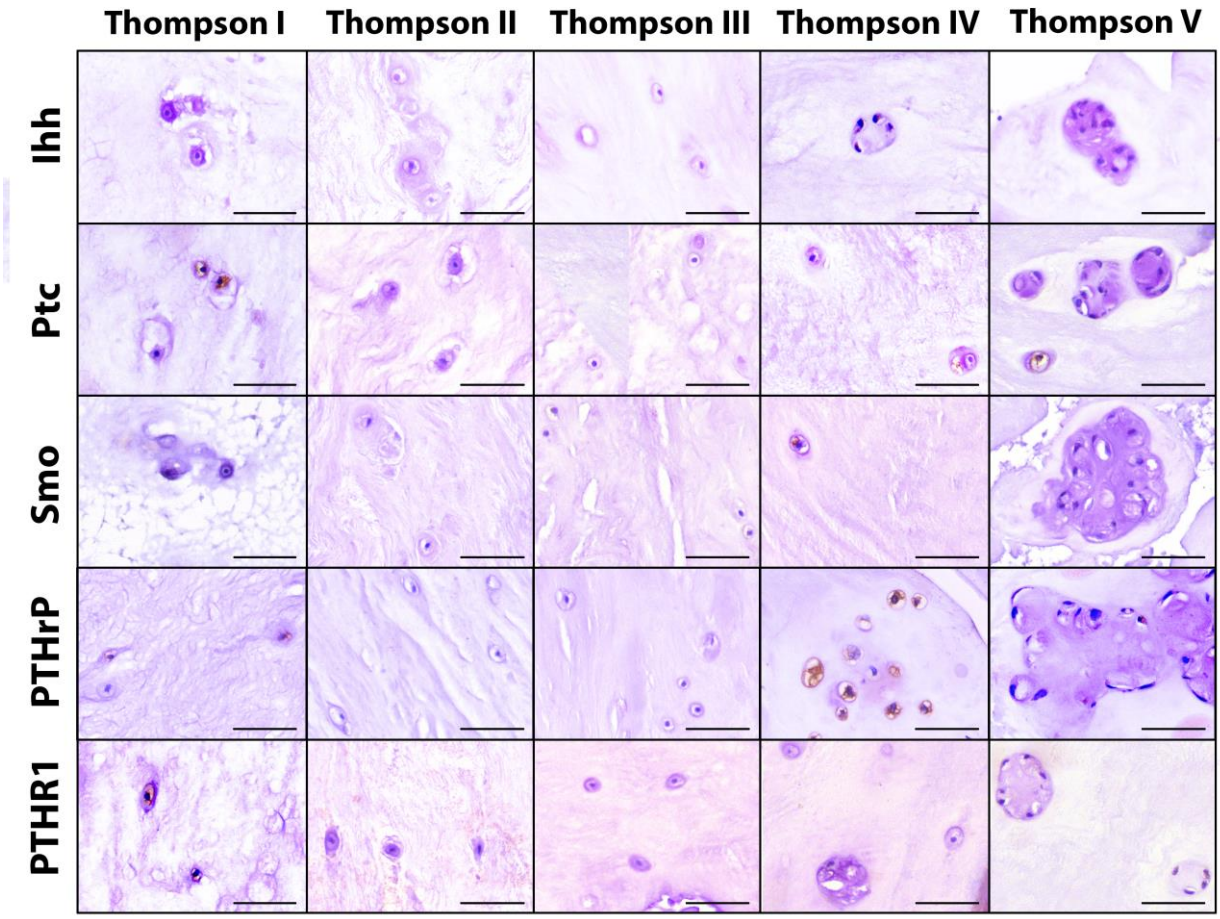

Figure 9. The expression of the proteins Parathyroid Hormone-related Peptide (PTHrP), PTHrP receptor type 1 (PTHR1), Indian Hedgehog (IHH), and the receptors of IHH (Patched (Ptc) and Smoothened (Smo)) in human nucleus pulposus (NP) tissue with different Thompson grades as determined by immunohistochemical staining. The grading scheme of Thompson ranging from a healthy intervertebral disc (grade I) to a severely degenerated

intervertebral disc (grade V). Healthy human NP tissue (Thompson grade I) contains notochordal cells (NCs) and chondrocyte-like cells (CLCs), while degenerated human NP tissue (Thompson grade II to V) contains only chondrocyte-like cells (CLCs). During severe degeneration of human NP tissue (Thompson grade IV and V) clusters of CLCs are formed. The CLC clusters become larger when degeneration progressed from Thompson grade IV to V. The scale bar indicates 50 µm.

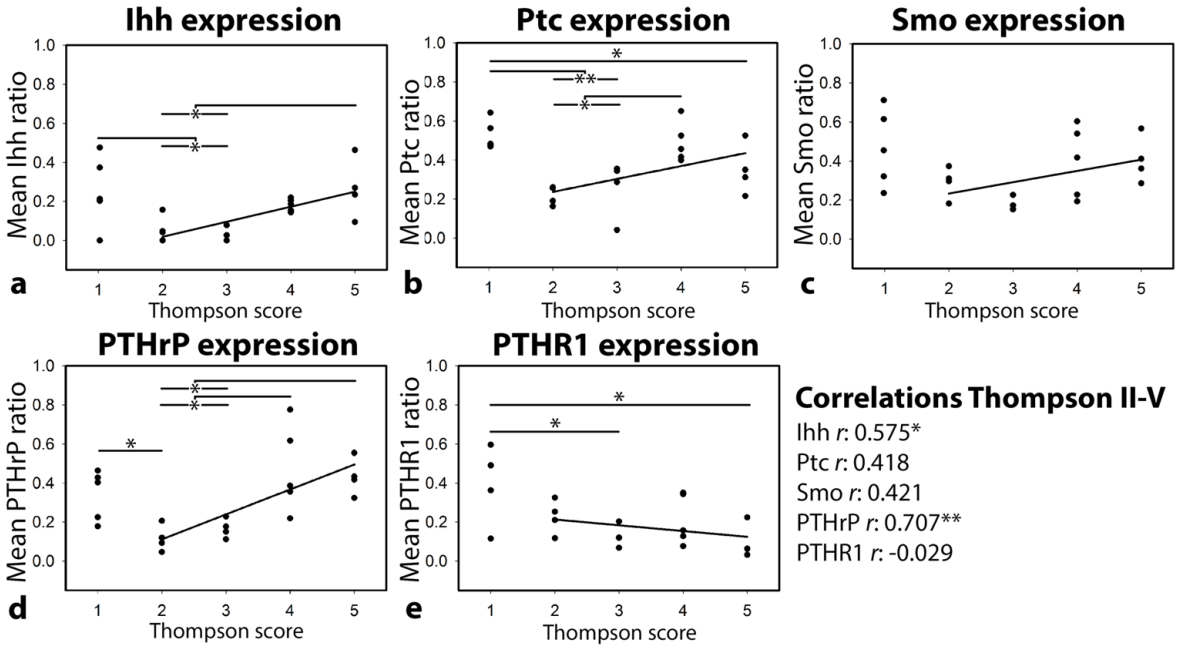

Figure 10. The PTHrP, IHH, Ptc, and Smo protein expression increased during IVD degeneration in nucleus pulposus (NP) tissue. (**a,b,c,d,e**) The expression of the protein Parathyroid hormone-related peptide (PTHrP), PTHrP receptor type 1 (PTHR1), Indian Hedgehog (IHH), and the IHH receptors Patched (Ptc) and Smoothened (Smo) in human NP tissue of different Thompson grades. Each symbol represents NP tissue of one particular human donor with its corresponding Thompson grade. The grading scheme of Thompson ranging from a healthy intervertebral disc (grade I) to a severely degenerated intervertebral disc (grade V). * $p<0.05$; ** $p<0.01$; *** $p<0.001$ (significance indicated changes to related Thompson grade); n=22 IVD samples derived from 22 human donors.

4.2. *In vitro* effects of PTHrP and IHH on canine NPCs derived from CD breeds

All canine NPC micro-aggregates contained a low GAG and DNA content (**Figure 11a,d**). On day 0, the DNA content of the micro-aggregates was significantly higher than after 28 days of control, 10^{-8} M PTHrP, 10^{-7} M PTHrP, 0.1 µg/mL IHH, and 1 µg/mL IHH treatment (p<0.001). The DNA content of the 10^{-7} M PTHrP-treated micro-aggregates was mild, but significantly lower than the DNA content of the control-treated micro-aggregates (p<0.001; **Figure 11d**). In contrast, there were no significant differences detected between the GAG content of the micro-aggregates (**Figure 11a**). The GAG release of the micro-aggregates was highest in the control micro-aggregates and 10^{-8} M PTHrP and 10^{-7} M PTHrP treatment induced a lower GAG release compared with the controls (p<0.01; **Figure 11b**). The total GAG production (GAG content of the micro-aggregate + GAG release in the medium) was significantly lower in the 10^{-8} M PTHrP- and 10^{-7} M PTHrP-treated micro-aggregates compared with the control micro-aggregates (p<0.01; **Figure 11c**). The GAG content corrected for the DNA content of the 10^{-7} M PTHrP-treated micro-aggregates (p<0.001) and the 1 µg/mL IHH-treated micro-aggregates (p<0.01) was significantly higher than in the control micro-aggregates (**Figure 11e**). In addition, the low GAG content was confirmed with the Safranin O/Fast Green staining, since this staining for the proteoglycans in the canine NPC micro-aggregates of all the culture conditions was weakly positive (**Figure 12**).

The expression of only two genes was significantly affected by treatment. The gene expression level of the ECM anabolic gene *COL1A1* was significantly higher in the control micro-aggregates compared with micro-aggregates treated with 10^{-7} M PTHrP, 0.1 µg/mL IHH, and 1 µg/mL IHH at 24 hours (p<0.05; **Figure 13**). Also there was a significantly higher gene expression level of *COL1A1* in micro-aggregates treated with 10^{-8} M PTHrP compared with the micro-aggregates treated with 10^{-7} M PTHrP, 0.1 µg/mL IHH, and 1 µg/mL IHH (p<0.05). The expression level of the PTHrP-IHH signaling gene *Ptc* was significantly higher in micro-aggregates treated with 1 µg/mL IHH compared with the control micro-aggregates at 24 hours (p<0.001). Also, there was a significantly higher gene expression level of *Ptc* in micro-aggregates treated with 1 µg/mL compared with micro-aggregates treated with 10^{-8} M PTHrP and 10^{-7} M PTHrP (p<0.01) and 0.1 µg/mL IHH (p<0.05). The expression levels of *ACAN*, *ADAMTS5*, *BAX*, *BCL2*, *CASP3*, *CCDN1*, *COL2A1*, *FOXF1*, *GLI1*, *GLI2*, *GLI3*, *ID1*, *IHH*, *KRT8*, *KRT18*, *KRT19*, *MMP13*, *PAI1*, *PTHRP*, *RUNX2*, *SMO*, *SOX9*, *TIMP1*, and *VEGF* were not statistically different between the conditions (**Figure 23, Figure 24,** and **Figure 25** in appendix). Gene expression levels of the ECM matrix anabolism gene *COL10A1*, PTHrP-IHH signaling genes *PTHR1* and *IHH*, and NP marker *T* could not be detected in the canine NPC micro-aggregates of all the different treated micro-aggregates.

If *PTHR1* was not expressed at gene expression level and the PTHR1 protein was not present, than PTHrP could not have exerted any effect on the canine NPC micro-aggregates. Therefore, immunohistochemistry for PTHR1 was performed and demonstrated a positive staining in two treatment micro-aggregates: 10^{-7} M PTHrP and 1 µg/mL IHH (**Figure 14**). However, there was no staining visible in the control and 0.1 µg/mL IHH-treated micro-aggregates. The 10^{-8} M PTHrP-treated micro-aggregate was not available, because the micro-aggregate was lost during processing.

Taken together, these data show that massive canine NPC cell death occurred in the current setup. In conclusion, this experimental setup could not be used for testing the effect of PTHrP and IHH on NPCs, and therefore a new experimental design was created.

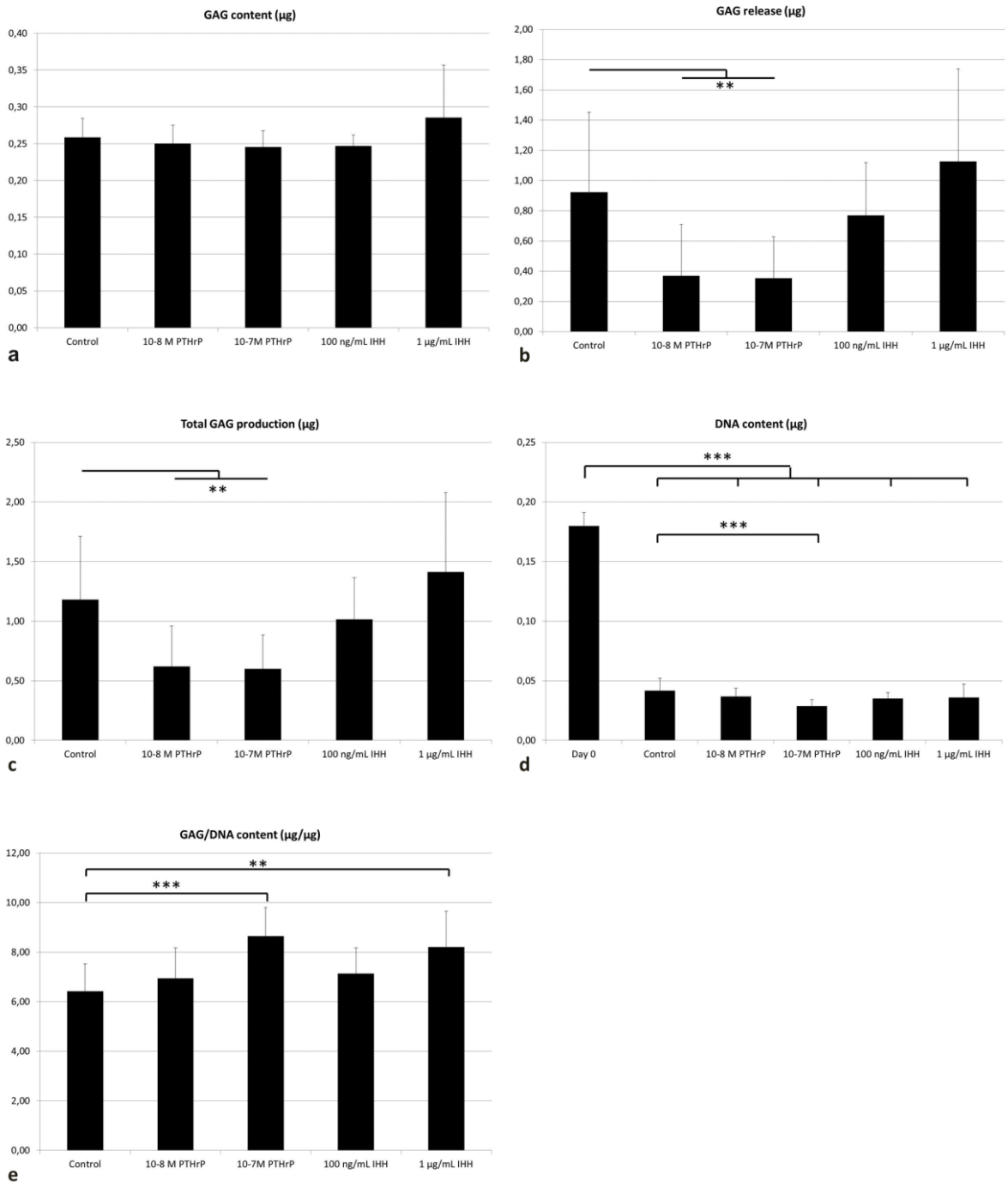

Figure 11. Canine nucleus pulposus cell (NPC) micro-aggregates with 10^{-7} M Parathyroid Hormone-related peptide (PTHrP) supplemented culture medium and 1 µg/mL Indian Hedgehog (IHH) supplemented culture medium contained a lower GAG/DNA content in comparison to the micro-aggregates treated with chondrogenic differentiation culture medium (control). Additionally, the canine NPC micro-aggregates with PTHrP supplemented culture medium (10^{-8} M and 10^{-7} M) release less GAGs in comparison to the control culture medium, as consequence the total GAG production is also lower in canine NPC micro-aggregates with PTHrP supplemented culture medium ((10^{-8} M and 10^{-7} M). **(a,d,e)** The GAG content, GAG release, total GAG production, DNA content, and GAG/DNA content (mean ± SD) of canine NPC micro-aggregates on day 14 cultured in control, 10^{-8} M PTHrP (10-8M PTHrP), 10^{-7} M PTHrP (10-7M PTHrP), 0.1 µg/mL IHH (0.1 µg/mL IHH), and 1 µg/mL IHH supplemented culture medium (1 µg/mL IHH) in hypoxia (5% O_2). *n*=6 in duplo per culture condition. ** p<0.01; ***p<0.001.

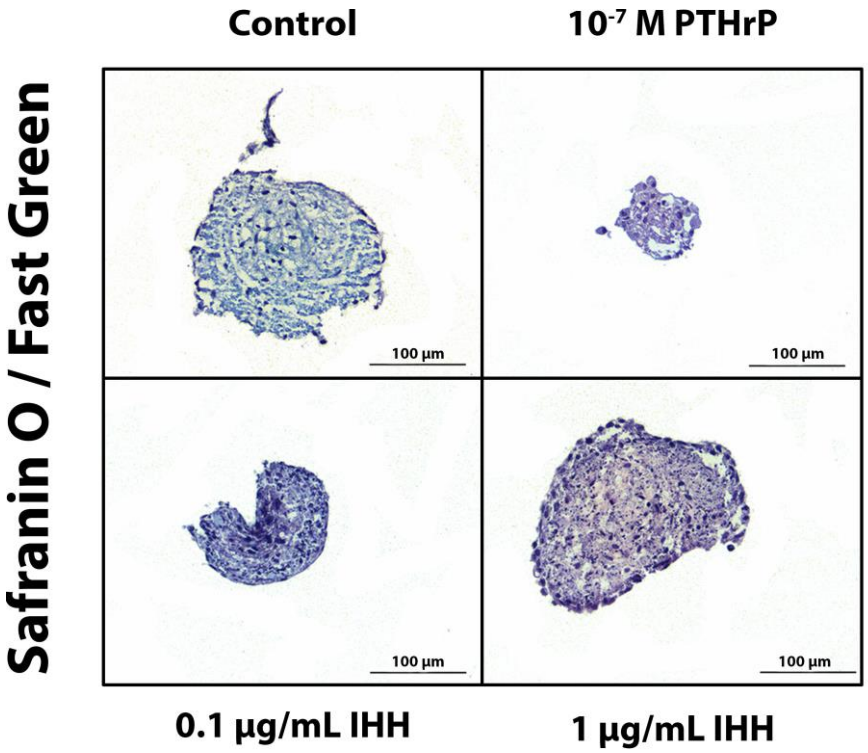

Figure 12. Canine nucleus pulposus cell (NPC) micro-aggregates cultured in Parathyroid hormone-related peptide (PTHrP) supplemented culture medium (10^{-7} M) or Indian hedgehog (IHH) supplemented culture medium (0.1 µg/mL or 1 µg/mL) induced very little GAG deposition. Safranin O/Fast Green staining of canine NP tissue cultured in micro-aggregates in chondrogenic differentiation culture medium (control), PTHrP culture medium with a concentration of 10^{-8} M or 10^{-7} M, and IHH culture medium with a concentration of 0.1 µg/mL or 1 µg/mL for 14 days in hypoxia (5% O_2). Red staining indicates GAG-rich matrix deposition.

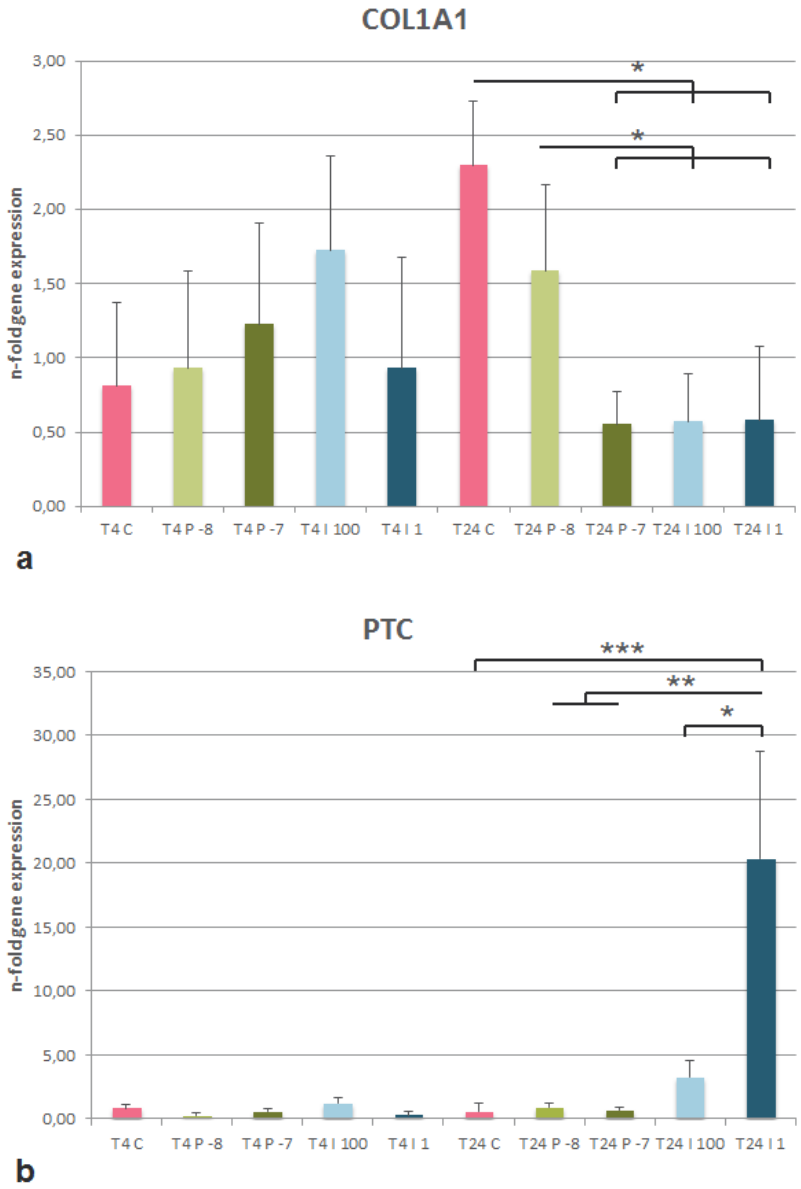

Figure 13. The gene expression level of the extracellular matrix (ECM) anabolic gene *COL1A1* is lower in the micro-aggregates treated with 10^{-7} M Parathyroid hormone-related peptide (PTHrP), 0.1 µg/mL Indian hedgehog (IHH), and 1 µg/mL IHH in comparison with the control- and 10^{-7} M PTHrP-treated micro-aggregates after 24 hours of treatment. The gene expression level of the PTHrP-IHH signaling gene *Ptc* is highest in the 1 µg/mL IHH-treated micro-aggregates at 24 hours. **(a,b)** Gene expression levels of the ECM anabolic *COL1A1* gene, and the PTHrP-IHH signaling *Ptc* gene after 4 and 24 hours of treatment with 10^{-8} M PTHrP (P-8), 10^{-7} M PTHrP (P-7), 0.1 µg/mL IHH (I0.1), and 1 µg/mL IHH (I1) in hypoxia (5% O_2). *n*=6 in duplo per culture condition; * $p<0.05$; ** $p<0.01$; *** $p<0.001$.

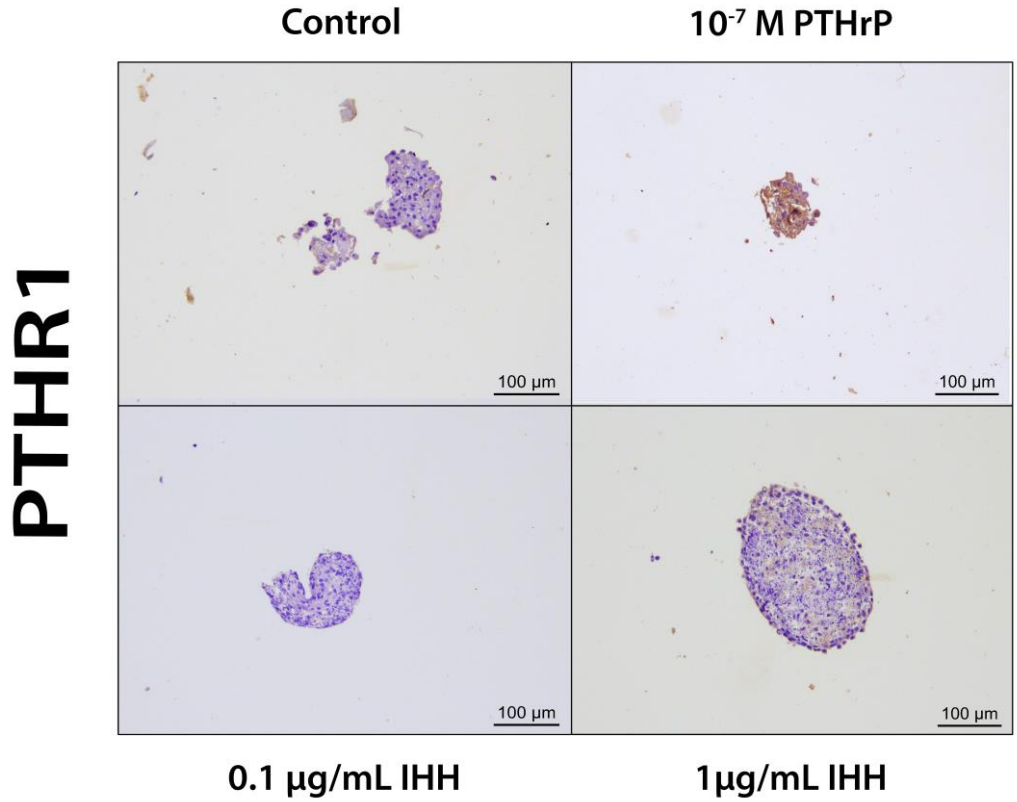

Figure 14. The protein PTHR1 was present in canine nucleus pulposus cell (NPC) micro-aggregates that were cultured in Parathyroid hormone-related peptide (PTHrP) supplemented culture medium (10^{-7} M) and Indian hedgehog (IHH) supplemented culture medium (1 µg/mL). PTHR1 immunohistochemistry of canine NP tissue cultured in micro-aggregates in chondrogenic differentiation culture medium supplemented with 10 ng/mL TGF-ß$_1$ (control), PTHrP culture medium supplemented with a concentration of 10^{-7} M, and IHH cultured medium supplemented with a concentration of 0.1 µg/mL or 1 µg/mL for 14 days in hypoxia (5% O_2). Brown staining indicates the presence of the PTHR1 protein.

4.3. *In vitro* effects of hypertrophic induction medium on canine NPCs

The collagen type X immunohistochemistry (**Figure 15**) and the Alizarin Red staining (data not shown) showed no positive staining result in the NPC micro-aggregates of all the culture conditions. Also PTHR1 immunohistochemistry showed no positive staining in the C-NX and C-HX treated micro-aggregates (**Figure 16**). However, the conditions C7H21-NX, C7H21-HX, C14H14-NX, and C14H14-HX showed a positive PTHR1 staining in the NPC micro-aggregates, which indicated that prehypertrophy was induced in the NPC micro-aggregates. There was a staining intensity difference between the normoxic and hypoxic conditions: the normoxic micro-aggregates contained more PTHR1 than the hypoxic micro-aggregates.

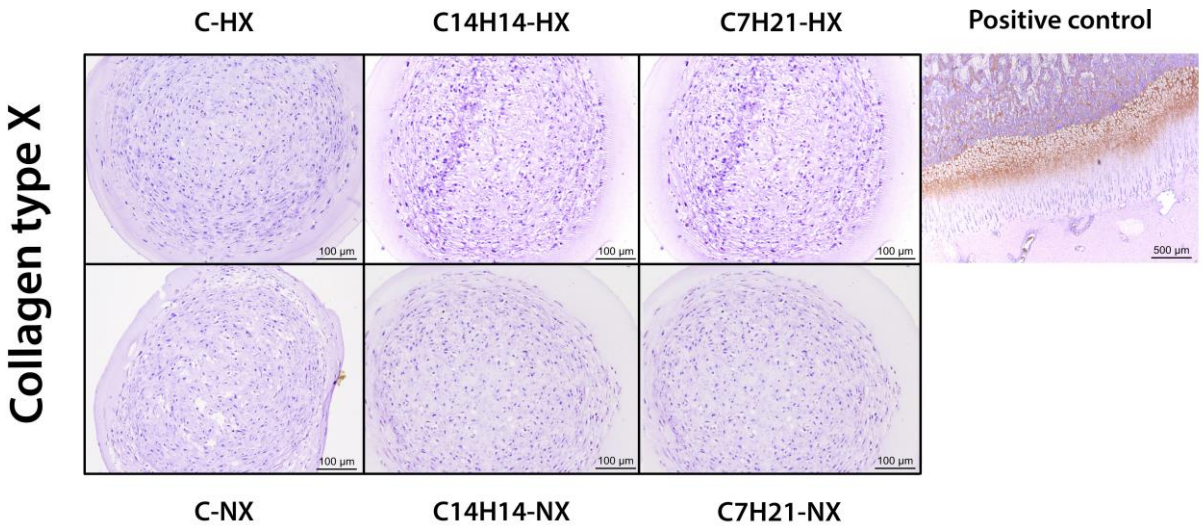

Figure 15. The hypertrophic collagen type X protein is not expressed in canine nucleus pulposus cell (NPC) micro-aggregates that were cultured in chondrogenic differentiation culture medium supplemented with 10 ng/mL TGF-ß$_1$ (C-HX or C-NX), or hypertrophic induction medium for 14 days (C14H14-HX or C14H14-NX), or hypertrophic induction medium for 21 days (C7H21-HX or C7H21-NX) in hypoxia (5% O_2; HX) or normoxia (21% O_2; NX). Brown staining indicates the presence of the collagen type X protein.

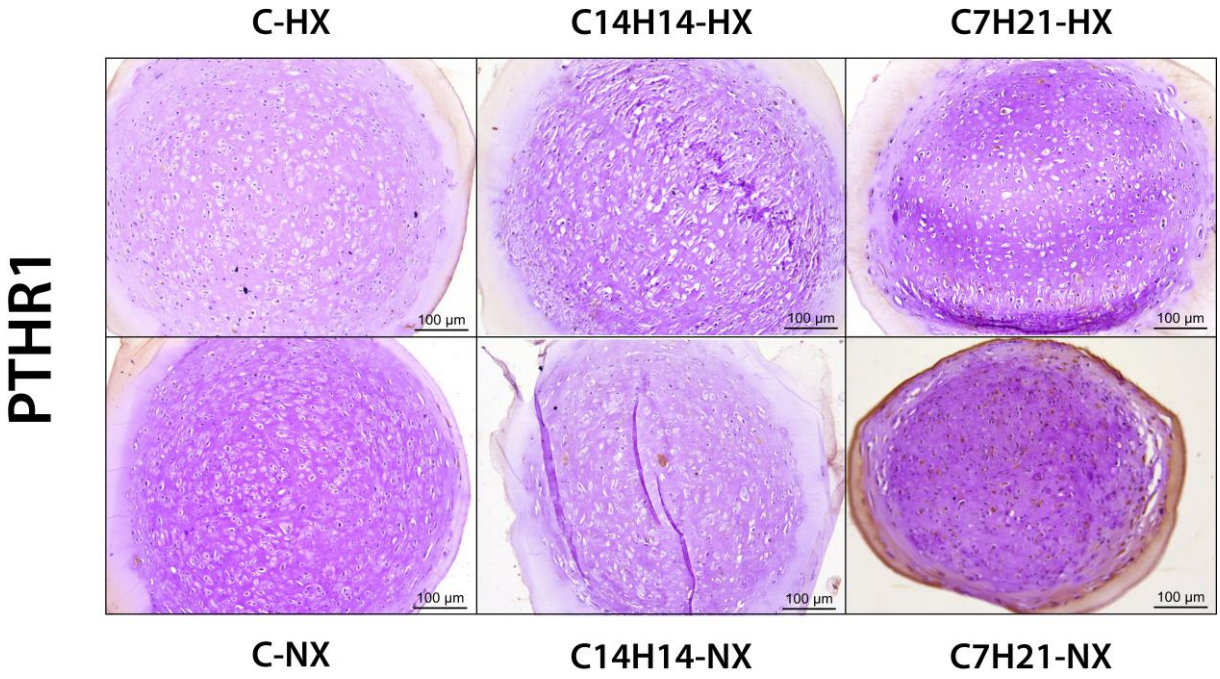

Figure 16. The prehypertrophic PTHR1 protein is present in the nucleus pulposus cell (NPC) micro-aggregates that were treated with hypertrophic induction medium for 14 days (C14H14) or 21 days (C7H21) in hypoxia (5% O_2; HX) and normoxia (21% O_2; NX). PTHR1 is more strongly expressed in normoxia than in hypoxia. In normoxia, PTHR1 is most strongly expressed in canine NPCs that were treated with hypertrophic induction medium for 21 days (C7H21-NX). The NPC micro-aggregates that were treated with chondrogenic differentiation culture medium supplemented with 10 ng/mL TGF-ß$_1$ in hypoxia (C-HX) and normoxia (C-NX) express no PTHR1 protein.

4.4. *In vitro* effects of PTHrP and IHH on prehypertrophic canine and human NPCs

The total GAG production (GAG content + GAG release in the medium) was lower in the canine and human NPC micro-aggregates that were treated with hypertrophic induction medium (with or without supplementation of PTHrP and IHH) than in those treated with chondrogenic differentiation culture medium supplemented with 10 ng/mL TGF-β_1 (p<0.001 or p<0.01; **Figure 17c** and **Figure 18c**). In addition, the total GAG production did not differ between canine and human NPC micro-aggregates that were treated with hypertrophic induction medium alone and NPC micro-aggregates that were supplemented with PTHrP or IHH. The DNA content of the canine and human micro-aggregates showed no significant differences between the different conditions (**Figure 17d** and **Figure 18d**). In canines, the GAG content corrected for the DNA content was significantly higher in the micro-aggregates treated with chondrogenic differentiation culture medium supplemented with TGF- β_1 than in all other conditions (hypertrophic induction medium (p<0.01), PTHrP (10^{-8} M and 10^{-7} M; p<0.001), and IHH (0.1 µg/mL and 1 µg/mL; p<0.05); **Figure 17e**). In humans, the GAG content corrected for the DNA content was significantly higher in the micro-aggregates treated with chondrogenic differentiation culture medium supplemented with 10 ng/mL TGF- β_1 than in the micro-aggregates treated with hypertrophic induction medium supplemented with 1 µg/mL IHH (p<0.05; **Figure 18e**). However, the GAG content corrected for the DNA content in the micro-aggregates treated with hypertrophic induction medium alone or supplemented with PTHrP (10^{-8} M and 10^{-7} M) or 0.1 µg/mL IHH were not significantly different from the micro-aggregates treated with chondrogenic differentiation culture medium.

No positive collagen type X staining was observed in the canine and human NPC micro-aggregates of all the culture conditions (data not shown). However, the Alizarin Red staining did show positive staining results in the canine and human NPC micro-aggregates. Not only canine donor C4 (**Figure 19**) but also human donor H6 (**Figure 20**) showed a strong positive staining result in the 1 µg/mL IHH-treated NPC micro-aggregates. In contrast to the negative staining results in the canine NPC micro-aggregates that were treated with chondrogenic differentiation culture medium supplemented with TGF-β_1, there was a positive staining result visible in the human NPC micro-aggregates of donor H6 that were treated with chondrogenic differentiation culture medium supplemented with TGF- β_1 (**Figure 20**).

Gene expression in the human NPC micro-aggregates was too low to measure (data not shown). The ECM anabolic gene *COL2A1* was significantly lower expressed in the canine NPC micro-aggregates that were treated with chondrogenic differentiation culture medium supplemented with TGF- β_1 than the micro-aggregates that were treated with hypertrophic induction medium with or without supplementation of PTHrP or IHH (p<0.01 or p<0.05; **Figure 21b**). The hypertrophic induction medium with or without supplementation of PTHrP or IHH induced an increased expression of the ECM catabolism gene *ADAMTS5* in canine NPC micro-aggregates. However, this was only significantly higher in the 1 µg/mL IHH-treated canine micro-aggregates compared with the micro-aggregates treated with chondrogenic differentiation culture medium supplemented with TGF- β_1, probably due to a low amount of donors (n=6) that were used (**Figure 21a**). The gene expression levels of *ACAN*, BCL2, *CASP3, CCND1, COL1A1, GLI2, ID1, KRT8, MMP13, PAI1, RUNX2, SOX9,* and *TIMP1* were not statistically different between the different conditions (**Figure 26** in appendix). Gene expression levels of *BAX, COL10A1, FOXF1, GLI1, GLI3, IHH, KRT18, KRT19, PTC, PTHrP, PTHR1, SMO, T, and VEGF* could not be detected in the canine NPC micro-aggregates of all the different treated micro-aggregates.

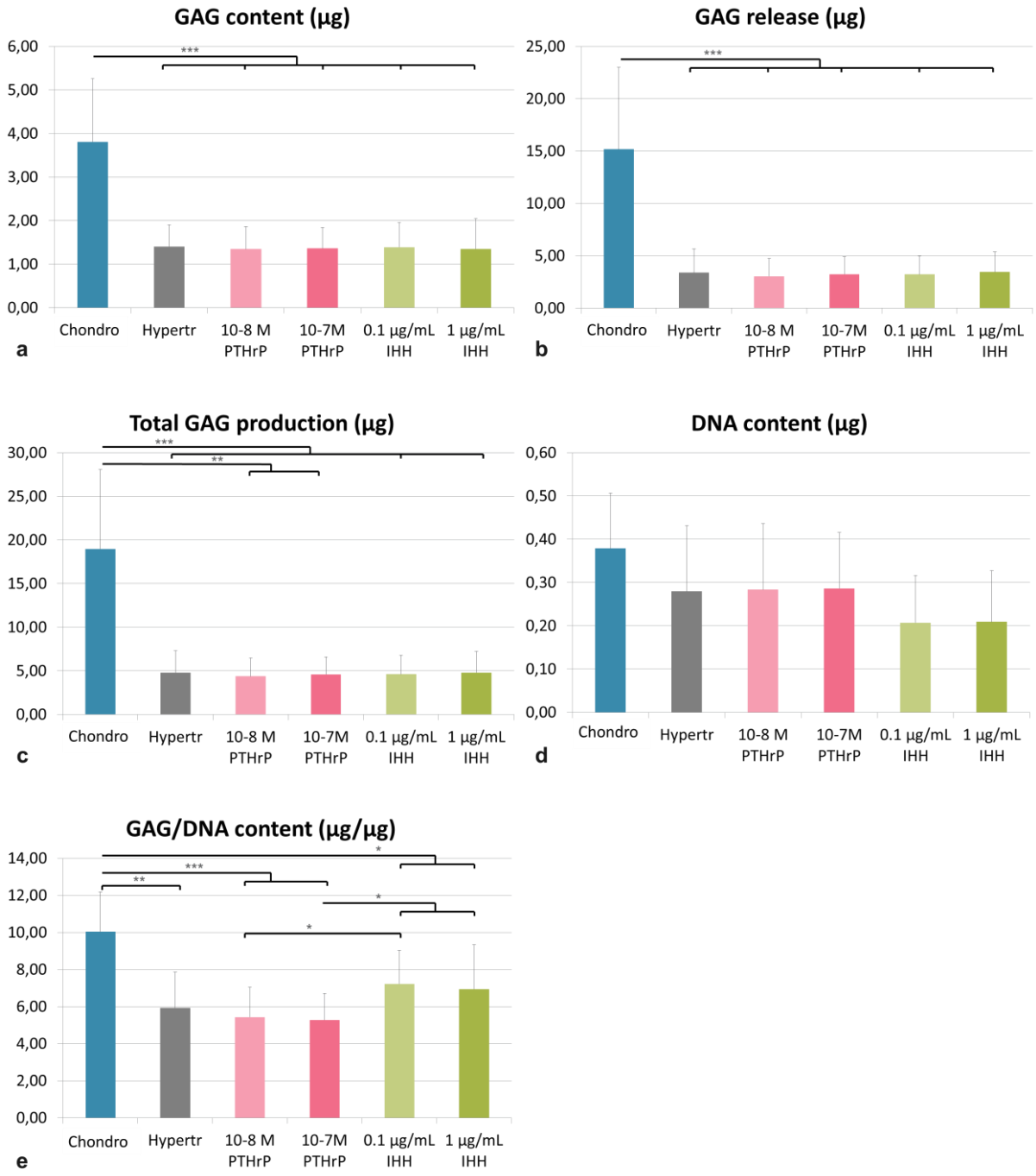

Figure 17. Treatment with hypertrophic induction medium significantly decreased the total GAG production of the canine nucleus pulposus cell (NPC) micro-aggregates compared with the chondrogenic differentiation culture medium supplemented with TGF-β_1 and supplementation with PTHrP or IHH did not augment GAG production in the hypertrophic NPCs. **(a-e)** The GAG content, GAG release in the medium, total GAG production, DNA content, and GAG/DNA content (mean ± SD) of canine NPC micro-aggregates on day 49 after culturing in chondrogenic differentiation culture medium supplemented with 10 ng/mL TGF-β_1, or hypertrophic induction medium, or hypertrophic induction medium supplemented with 10^{-8} M PTHrP, 10^{-7} M PTHrP, 0.1 µg/mL IHH, or 1 µg/mL IHH in normoxia (21% O_2). *n*=6 in duplo per culture condition; * $p<0.05$; ** $p<0.01$; *** $p<0.001$.

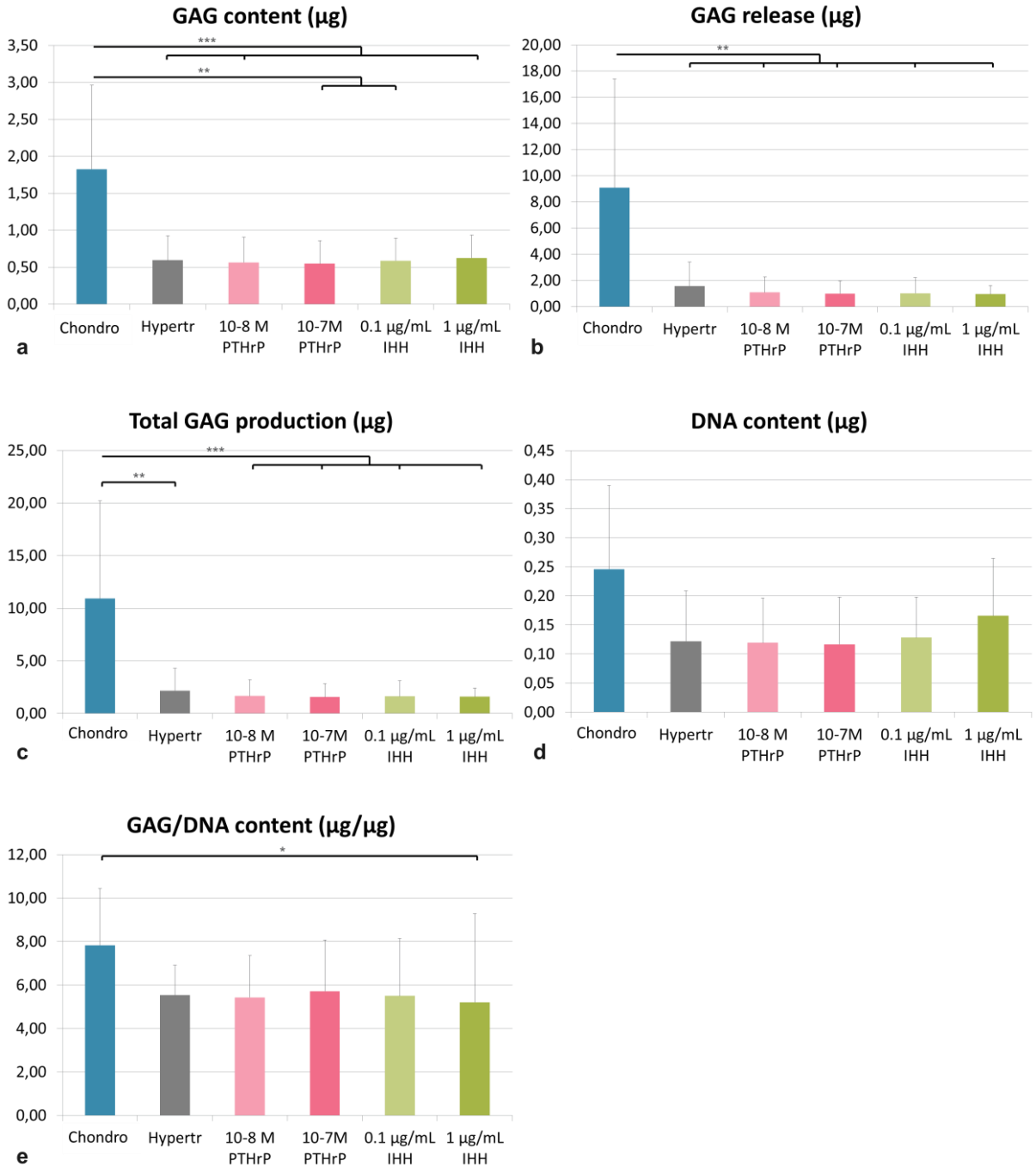

Figure 18. Treatment with hypertrophic induction medium significantly decreased total GAG production of the canine nucleus pulposus cell (NPC) micro-aggregates compared with the chondrogenic differentiation culture medium supplemented supplemented with TGF-β1 and supplementation with PTHrP or IHH did not augment GAG production in the hypertrophic NPCs. (**a-e**) The GAG content, GAG release in the medium, total GAG production, DNA content, and GAG/DNA content (mean ± SD) of human NPC micro-aggregates on day 49 after culturing in chondrogenic differentiation culture medium supplemented with 10 ng/mL TGF-β_1, or hypertrophic induction medium, or hypertrophic induction medium supplemented with 10^{-8} M PTHrP, 10^{-7} M PTHrP, 0.1 µg/mL IHH, or 1 µg/mL IHH in normoxia (21% O_2). *n*=6 in duplo per culture condition; * *p*<0.05; ** *p*<0.01; *** *p*<0.001.

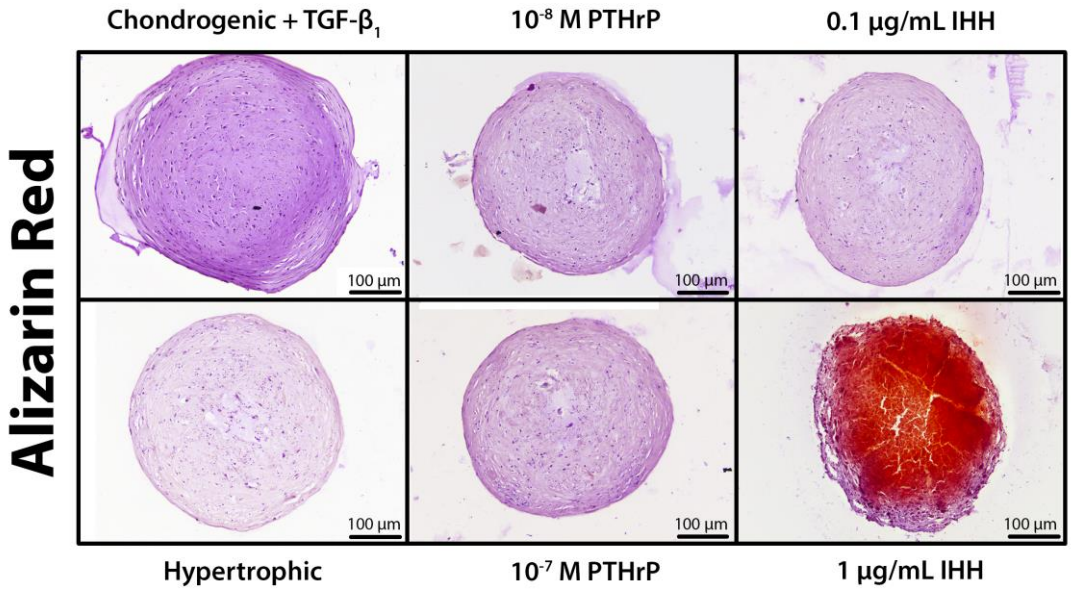

Figure 19. Hypertrophic induction medium supplemented with 1 µg/mL IHH induces calcification in canine nucleus pulposus cell (NPC) micro-aggregates derived from early degenerated canine intervertebral discs on day 49. The canine NPC micro-aggregates were cultured in chondrogenic differentiation culture medium supplemented with 10 ng/mL TGF-β_1, or hypertrophic induction medium (1 nM 3,3',5-triiodo-L-thyronine (T3), 10 mM β-glycerophosphate and 10^{-9} M dexamethasone), or hypertrophic induction medium supplemented with PTHrP (10^{-8} M or 10^{-7} M) or IHH (0.1 µg/mL or 1 µg/mL) for 49 days in normoxia (21% O_2). Red Alizarin Red S staining indicates calcium deposition.

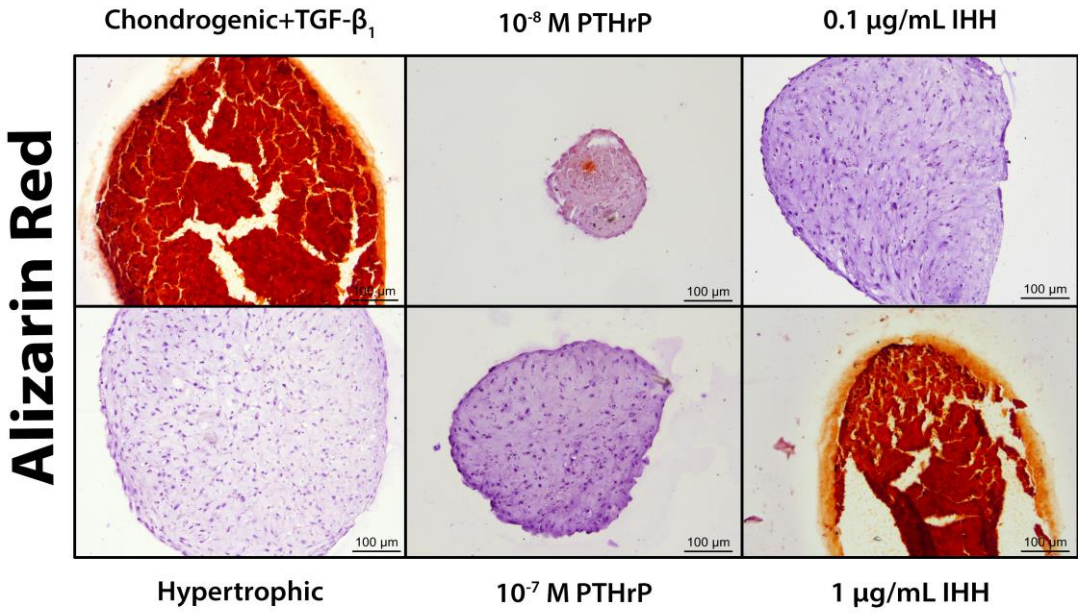

Figure 20. Hypertrophic induction medium supplemented with 1 µg/mL induced calcification in nucleus pulposus cell (NPC) micro-aggregates derived from early degenerated human intervertebral disc on day 49. The canine NPC micro-aggregates were cultured in chondrogenic differentiation culture medium supplemented with 10 ng/mL TGF-ß$_1$, or hypertrophic induction medium (1 nM 3,3',5-triiodo-L-thyronine (T3), 10 mM ß-glycerophosphate, and 10^{-9} M dexamethasone), or hypertrophic induction medium supplemented with Parathyroid hormone-related peptide (PTHrP: 10-8 M or 10-7 M) or IHH (0.1 µg/mL or 1 µg/mL) for 49 days in normoxia (21% O_2). Red Alizarin Red S staining indicates calcium deposition.

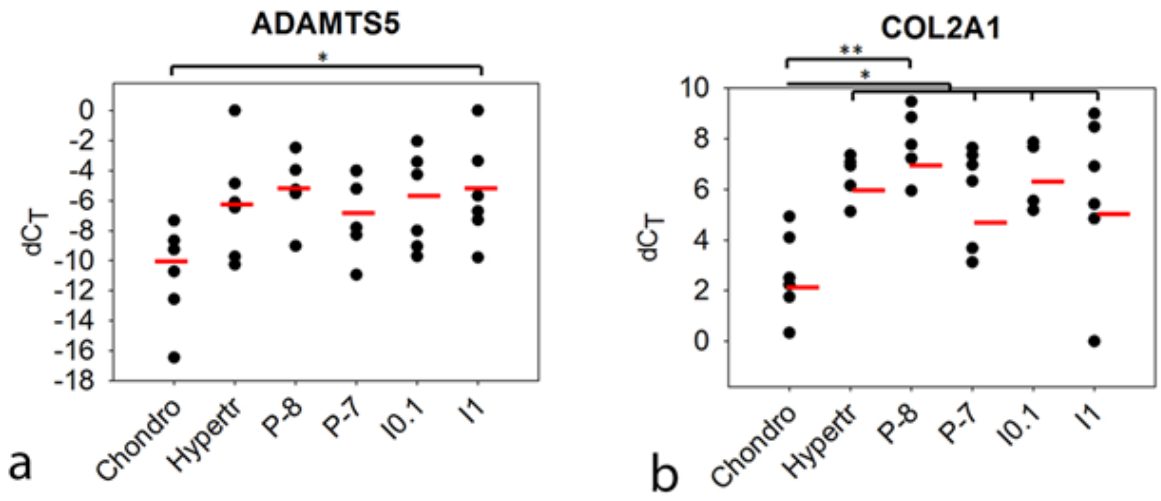

Figure 21. Hypertrophic induction medium with or without supplementation of Parathyroid hormone-related peptide (PTHrP: 10^{-8} M or 10^{-7} M) or Indian hedgehog (IHH: 0.1 µg/mL or 1 µg/mL) generates *COL2A1* mRNA expression and the hypertrophic induction medium supplemented with 1 µg/mL IHH induces *ADAMTS5* mRNA expression in canine NPC micro-aggregates **(a,b)** The ΔC_T-values, which are relative measures of the concentration of the target gene in the Real-Time quantitative Polymerase Chain Reaction analysis, of the extracellular matrix (ECM) anabolic gene *COL2A1* and the ECM catabolism gene *ADAMTS5* in canine NPC micro-aggregates at day 35 in normoxia (21% O_2). Each black dot represents one particular canine donor and each red line represents the mean of the 6 canine donors of one specific culture condition. *n*=6 in duplo per culture condition; * *p*<0.05; ** *p*<0.01.

5. Discussion

IVD degeneration is a common disease in dogs and humans. Current treatment options do not lead to repair, so there is need for treatments resulting into functional IVD restoration. Previous work indicated a positive correlation between IHH expression and OA (35,36), which is a process resembling IVD degeneration (29). In the process of OA IHH induces hypertrophy and mineralization (35,37,38). In contrast to IHH, PTHrP has been reported to have a protective role in the maintenance of articular chondrocytes and therefore promotes cartilage repair by inhibiting hypertrophy of articular chondrocytes in OA patients (21,23,39,40). While the role of PTHrP and IHH is well recognized in endochondral ossification and articular cartilage, not much information on the role of PTHrP and IHH in the IVD is available. Hence, understanding the role of PTHrP and IHH is crucial to further develop regenerative strategies for IVD degeneration. In order to do so, first, the protein expression of PTHrP, IHH and their receptors (PTHR1, Ptc, and Smo) was determined in human IVDs. The protein expression in canine IVDs was already investigated by our group (unpublished work). Second, canine and human NPCs derived from early degenerated IVDs were cultured in three-dimensional (3D) micro-aggregates to investigated the effect of PTHrP and IHH supplementation on these cells in terms of ECM production.

PTHrP-IHH signaling is active in healthy and degenerated IVDs

PTHrP and IHH are both required for normal skeletal development and for regulating the maintenance of articular cartilage (41,42).

During endochondral ossification, PTHrP serves to maintain the survival and chondrogenesis of proliferating chondrocytes and slows the terminal differentiation from hypertrophy to mineral deposition to eventually apoptosis (41). Periarticular proliferating chondrocytes express PTHrP and downregulate the expression of IHH. IHH produced by prehypertrophic chondrocytes initiate hypertrophic cartilage formation and stimulates PTHrP expression, which keeps the chondrocytes in a proliferating state (21,41). This negative feedback loop regulates the balance between proliferation and (terminal) differentiation of chondrocytes, which ensures orderly bone formation (21).

PTHrP and IHH are also involved in the maintenance of articular cartilage and in OA development. During OA development, articular chondrocytes are known to undergo the same process of terminal differentiation as they do in endochondral ossification (36,41,43). Additionally, previous work indicated a positive correlation between IHH expression and OA, which is a process resembling IVD degeneration (35,36). In the process of OA IHH promotes hypertrophy and mineralization (44), while PTHrP and PTH suppresses these processes (23,41). PTHR1 expression is downregulated in OA chondrocytes (45).

Based on the results from the above mentioned studies, we hypothesized that PTHrP expression would be decreased during IVD degeneration, while IHH expression would be increased during IVD degeneration. In contrast to our hypothesis, in the current study we show that the protein expression of both PTHrP and IHH decreased from healthy to early degenerated human IVDs and increased from early to severely degenerated human IVDs (**Figure 10**). In line with these results, unpublished work by our group showed that PTHrP and IHH expression decreased from healthy to early degenerated canine IVDs and increased from early to severely degenerated canine IVDs (**Figure 22**). In our opinion, there are two explanations for these results: PTHrP either aids an attempt at

regeneration or it induces /facilitates degeneration. Altogether, PTHrP and IHH expression is present in the healthy and degenerated IVD and this indicate that PTHrP and/or IHH signaling might play a role in IVD degeneration or regeneration.

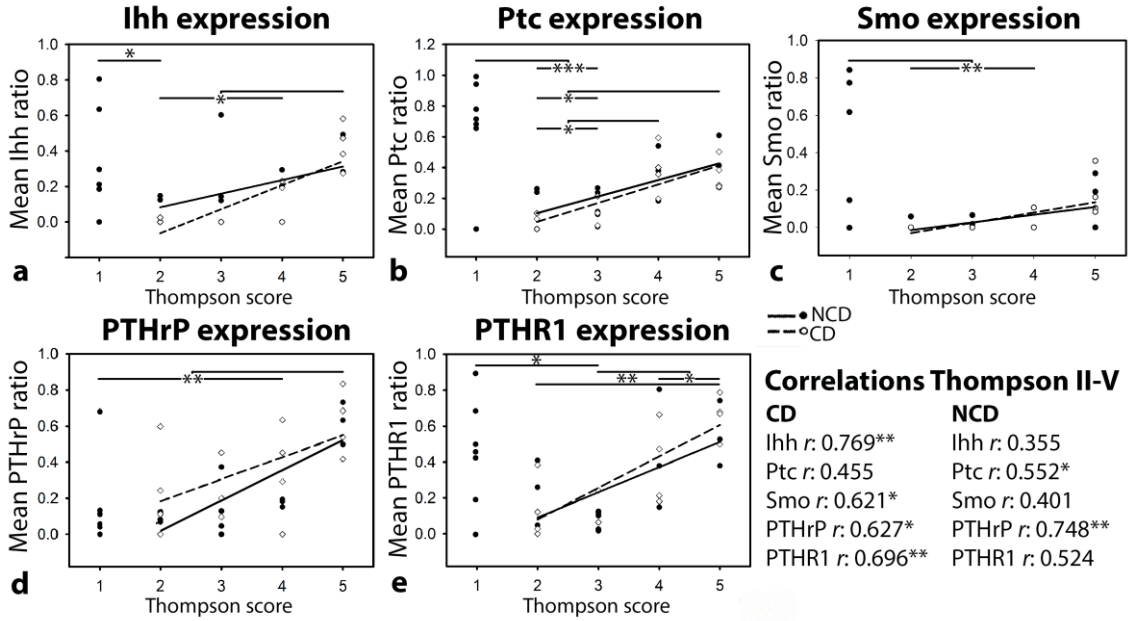

Figure 22. The protein expression of Parathyroid hormone-related peptide (PTHrP), PTHrP receptor 1 (PTHR1), Indian hedgehog (IHH), and the IHH receptors Patched (Ptc) and Smoothened (Smo) in canine intervertebral discs with different degeneration grades, ranging from healthy (Thompson grade I) to severely degenerated (Thompson grade V). * p<0.05; ** p<0.01; *** p<0.001; CD: Chondrodystrophic dog breeds; NCD: non-chondrodystrophic dog breeds.

To establish the role of PTHrP and IHH, we cultured canine and human NPCs from degenerated IVDs in 3D micro-aggregates. This 3D cell culture model, which contains 35,000 NPCs per micro-aggregate, was used since a more *in vivo* resembled situation of IVD degeneration was created regarding cellular communication and matrix interactions for cell growth and differentiation. Thus, 3D *in vitro* micro-aggregate cell culture models better mimic tissue physiology while two-dimensional (2D) cell culture does not adequately take into account the natural 3D environment of cells, could change the phenotype of the cells into a fibroblast-like phenotype, and could alter the cellular response *in vitro* which would result in misleading data for *in vivo* responses (46-49). Furthermore, we used micro-aggregates instead of pellets because micro-aggregates contains fewer cell layers (35,000 cells) than pellets (200,000 cells) and therefore micro-aggregates have a better nutrient supply to the inner cells of the 3D structure than pellets have.

In the current study, in total, three different 3D culture experiments were performed; one of them was a pilot study (experiment A (**section 3.2.** and **section 4.2.**), pilot study (**section 3.3.** and **section 4.3.**), and experiment B (**section 3.4.** and **section 4.4.**).

PTHrP and IHH do not induce GAG deposition in canine NPCs

Having established that protein expression of PTHrP and IHH is present in the healthy and degenerated IVD, we wanted to define the role of PTHrP and IHH in IVD degeneration. Based on the role of PTHrP and IHH in endochondral bone formation and articular cartilage, it is tempting to hypothesize that IHH also promotes degenerative effects in the degenerated IVD by promoting hypertrophy and mineralization, while PTHrP induces regenerative effects in the degenerated IVD by stimulating proliferation, inhibiting apoptosis, and suppressing hypertrophy and mineralization. To determine the effect of PTHrP and IHH on NPC ECM production, we performed a 3D cell culture experiment with canine NPCs from early degenerated IVDs, cultured in basal culture medium supplemented with PTHrP (10^{-8} or 10^{-7} M) or IHH (0.1 or 1 µg/mL) for 14 days (experiment A). The concentration of 10^{-8} M PTHrP was chosen since earlier research has already proven that this concentration induced inhibition of hypertrophic differentiation in growth plate chondrocytes (24). The concentration of 0.1 µg/mL IHH was based on a study that the manufacturer referred to, *Handorf et al.* (2015), which concluded that IHH plays a role in promoting hypertrophy during differentiation in human bone marrow stromal cell pellet cultures (30). Additionally, two higher concentrations of PTHrP (10^{-7} M) and IHH (1 µg/mL) were chosen if the initial concentrations would have been too low to induce effects.

Moreover, because the intervertebral disc is the largest avascular structure in the body and the microenvironment of the NP is characterized by a very low oxygen tension (50), we decided to perform this experiment in an hypoxic environment (5% O_2). *In vitro* studies indicated that NPCs could survive at low oxygen tension, provided that glucose was present, without a significant loss of cell viability (51,52). In our study, all the canine NPC micro-aggregates contained a very low GAG and DNA content after 14 days of culture (**Figure 11**). Consequently, the NPC micro-aggregates were very small. The Safranin O/Fast Green staining, used to detect proteoglycans, showed little GAGs in the canine NPC micro-aggregates (**Figure 12**). In short, our results indicate that PTHrP and IHH could not induce cell proliferation and ECM production in canine NPCs.

Also massive cell death occurred in the current setup, because the DNA content of the micro-aggregates was significantly lower after 14 days of control, 10^{-8} M PTHrP, 10^{-7} M PTHrP, 0.1 µg/mL IHH, and 1 µg/mL IHH treatment than on day 0 (**Figure 11**). The lack of a proper growth factor in our experiment could have explained the massive cell death. Because previous studies have shown that TGF-β can potentially affect ECM synthesis by increasing collagen type II and aggrecan synthesis, decreasing the production of proteolytic enzymes, and increasing the production of protease inhibitors (53,54), we decided to supplement TGF-β to the chondrogenic differentiation culture medium in our new pilot study to create a condition that should show increased GAG production in the NPCs.

Additionally, immunohistochemistry for PTHR1 was performed in experiment A because we were not sure if PTHR1 protein expression was present as we could not detect any PTHR1 mRNA in all the differently treated canine NPC micro-aggregates (**Figure 14**). If PTHR1 expression was not present, PTHrP could not have exerted any effects on the canine NPC micro-aggregates. The immunohistochemistry of PTHR1 demonstrated positive staining results in the 10^{-7} M PTHrP- and 1

µg/mL IHH-treated micro-aggregates which confirmed that PTHrP could have exerted effects on the NPC micro-aggregates.

As a final point, the results of experiment A showed that gene expression levels of *Ptc* were upregulated after a 24 hour treatment with 1 µg/mL IHH in comparison with the control group (**Figure 13**). This may indicated that Ptc is upregulated by IHH. In agreement with our results, previous work demonstrated that IHH also increases the expression of Ptc during bone formation (55,56). Thus, these results indicate that the 1 µg/mL IHH exerted an effect on the canine NPC micro-aggregates.

Taken together, PTHrP and IHH is present in healthy and degenerated IVDs, but they do not seem to affect ECM production and cell proliferation, thus PTHrP and IHH did not have an anabolic effect on the NPC micro-aggregates from early degenerated IVDs *in vitro*. Also, PTHrP and IHH could not counteract apoptosis and therefore, we wanted to determine if PTHrP and/or IHH have an effect on mineralization.

Hypertrophic induction medium induces prehypertrophy in canine NPC micro-aggregates

Having established that the protein expression of PTHrP and IHH is present in the degenerated IVD but did not affect the ECM production and cell proliferation or counteract apoptosis, we wanted to investigate the effect of PTHrP and IHH on hypertrophy and mineralization because IVD degeneration is associated with hypertrophic differentiation and calcification in the NP (32). Our aim was to redirect the NPC micro-aggregates towards an hypertrophic differentiation stage by supplementing hypertrophic induction medium in our pilot study.

In the pilot study, three elements were changed in comparison with experiment A. First, we added TGF-β to the chondrogenic differentiation culture medium. Second, we tried to induce hypertrophy by using hypertrophic induction medium. Lastly, we cultured the NPC micro-aggregates not only in an hypoxic environment but also in a normoxic environment to compare the different effects on the NPCs.

Previous work indicates that induction of chondrogenesis in MSCs is necessary, because without this, no hypertrophy was observed (31). Induction of chondrogenesis is accomplished by culturing human MSCs in a serum free chondrogenic differentiation culture medium, containing TGF-β and dexamethasone (57). *Mueller et al. (2008)* cultured human MSC pellets in chondrogenic differentiation culture medium for 14 days to induce predifferentiation, and thereafter hypertrophy was induced with 10 ng/mL TGF-β withdrawal, dexamethasone reduction (from 100 nM to 1 nM), and addition of 1 nM T3 (with or without β-glycerophosphate). After this, a distinct hypertrophic phenotype was seen. However, addition of these compounds alone did not induce hypertrophy (57). Also, *Gawlitta et al. (2012)* cultured MSC pellets in chondrogenic differentiation culture medium for 2.5 weeks and, thereafter, transferred to the hypertrophic induction medium consisting of DMEM, 1% ITS+ premix, 10^{-9} M dexamethasone, 10 mM β-glycerophosphate, 0.2 mM ASAP, Penicillin/Streptomycin, and 1 nM T3. They showed that hypertrophic differentiation was induced in chondrogenically predifferentiated MSC pellets (31). However, the results of the current pilot study on NPCs showed that collagen type X protein expression and calcification, both hypertrophic

markers, were absent (**Figure 15**). This contradiction is probably due to a difference in cell type (NPCs vs. MSCs). The prehypertrophic marker PTHR1, however, was present in the NPC micro-aggregates that were treated with hypertrophic induction medium (**Figure 16**). This indicates that the canine NPC micro-aggregates in our pilot study were in a prehypertrophic differentiation stage, but that we did not achieve a hypertrophic differentiation stage. Our hypothesis was that the NPC micro-aggregates were treated too short with hypertrophic induction medium to induce hypertrophy and thus to induce collagen type X expression and calcification.

Furthermore, a normoxic environment seems to play a role in the progression of hypertrophy. Normally, in a healthy IVD, the IVD contains a very low oxygen level vary from 1% to 5% because it is an avascular structure (50,58). However, during IVD degeneration the oxygen levels in the IVD increase due to blood vessel ingrowth (59). Several studies have demonstrated that MSCs or chondrocytes respond superior to normoxic than hypoxic culture conditions (31,60,61). For example, *Gawlitta et al. (2012)* focused on the effects of normoxic (20% O_2) and hypoxic (5% O_2) conditions on the progression of the hypertrophic differentiation of human MSCs in a cell culture for 4 weeks. The cultures of normoxic conditions seemed to be further advanced in hypertrophy than their hypoxic counterparts were. This was evidenced by greater areas of collagen type X expression, which is synthesized by hypertrophic chondrocytes, and matrix mineralization (31). In agreement with these studies, the results of our pilot study demonstrated also obvious stronger expression of PTHR1 in the canine NPC micro-aggregates cultured under normoxic conditions compared with the hypoxic conditions (**Figure 16**). However, as has been mentioned earlier, collagen type X protein expression and calcification were not visible under both normoxic and hypoxic conditions in our study, while the opposite was true in an earlier report of *Gawlitta et al. (2012)* who exclusively observed mineralization in hypertrophically stimulated, normoxic cultures (31). This contradiction is probably due to a difference in cell type. Another possible reason for a more advanced state of prehypertrophy in the normoxic conditions could be that the progression of prehypertrophy was delayed in hypoxic compared with normoxic conditions. In addition, *Gawlitta et al. (2012)* concluded that when oxygen levels were increased to a normoxic level in chondrocytes, reactive oxygen species (ROS) were generated and these ROS further enhance the hypertrophic differentiation of chondrocytes. So, generation of ROS might also enhance hypertrophic differentiation in our experiment.

In conclusion, we showed that prehypertrophy was successfully induced in the canine NPC micro-aggregates and that normoxic conditions seems to be more benefical for prehypertrophic differentiation of NPCs than hypoxic conditions.

Induction of calcifications by IHH occurred independently from collagen type X expression

Because our pilot study has already shown that NPC prehypertrophy was successfully induced and normoxic conditions seems to be more beneficial for prehypertrophic differentiation of NPCs than hypoxic conditions, we decided to perform a new experiment (experiment B). This time we cultured canine and human NPC micro-aggregates from early degenerated IVDs in chondrogenic differentiation culture medium supplemented with TGF-β_1, or hypertrophic induction medium, or hypertrophic induction medium supplemented with PTHrP (10^{-8} M or 10^{-7} M) or IHH (0.1 µg/mL or 1 µg/mL) for 49 days.

In this study, the total GAG production decreased after treatment with hypertrophic induction medium with or without supplementation of PTHrP or IHH in comparison to the chondrogenic differentiation culture medium supplemented with TGF-β_1 (**Figure 17** and **Figure 18**). In short, PTHrP and IHH did not induce GAG deposition in prehypertrophically differentiated canine and human NPCs. The low GAG production was supported by an increased *ADAMTS5* mRNA level in the NPC micro-aggregates treated with hypertrophic induction medium and with or without supplementation of PTHrP or IHH (**Figure 21**) because, in OA, *ADAMTS5* is responsible for aggrecan degradation in the ECM (62,63). Only the NPC micro-aggregates that were treated with 1 µg/mL IHH had a significantly higher *ADAMTS5* mRNA level in comparison to the micro-aggregates that were treated with chondrogenic differentiation culture medium supplemented with TGF-β_1. Although there was no other significant difference between the chondrogenic-treated micro-aggregates and the hypertrophic induced micro-aggregates (with or without supplementation of PTHrP or IHH), probably due to a low amount of donors (*n*=6), still the results indicate that *ADAMTS5* mRNA level increased.

Furthermore, collagen type X expression was not detected in our study (**section 4.4.**). This means that there was probably no hypertrophy induced because collagen type X expression is specifically expressed in hypertrophic chondrocytes (64,65). However, calcifications were visible in one canine donor (C4) and one human donor (H6), both treated with 1 µg/mL IHH (**Figure 19** and **Figure 20**). *Melrose et al. (2009)* also showed that calcification occurred independently from collagen type X expression in aged ovine IVDs (66). Important to mention is that donor C4 already had calcified IVDs during NPC harvesting so that calcium deposition could probably be more easily stimulated in this donor. In addition, our results showed that in donor H6 calcifications were visible in NPC micro-aggregates that were treated with chondrogenic differentiation culture medium supplemented with TGF-β_1. An explanation for this could be that TGF-β_1 is able to induce calcifications after 49 days of culture. In line with our thoughts, *Clark-Greuel et al. (2007)* reported that sheep aortic valve interstitial cells in culture progressively calcified over 14 days after the addition of TGF-β_1 through an apoptosis mediated process (67). However, in the other two canine (C5 and C6) and human donors (H4 and H5) of our experiment, there were no calcifications discernible at all. Possibly donor variation determined whether or not calcification is present. However, repetition of the experiment is necessary to gain more direct evidence and to elucidate the underlying mechanisms more clearly.

Moreover, *COL2A1* mRNA was significantly lower expressed in the canine NPC micro-aggregates that were treated with chondrogenic differentiation culture medium supplemented with TGF- β_1 than in the micro-aggregates that were treated with hypertrophic induction medium with or without supplementation of PTHrP or IHH (**Figure 21**). This result was against our expectations because earlier studies reported that proliferating chondrocytes in the growth plate express high levels of collagen type II, whereas collagen type II diminish progressively during terminal differentiation (68,69). However, in line with our results, *Tryfonidou et al. (2011)* reported that *COL2A1* mRNA was detected in many prehypertrophic and hypertrophic murine chondrocytes, since terminally differentiating growth plate chondrocytes will probably re-initiate or will never stop expressing *COL2A1* (70). In addition, another study demonstrated that *COL2A1* transcripts were also present in human hypertrophic chondrocytes (71). However, we could not compare this finding with the *COL2A1* mRNA levels in the human NPC micro-aggregates of our study because the *COL2A1* mRNA levels were too low to measure.

Taken together, our results showed that IHH is able to induce calcifications in prehypertrophic canine and human NPCs and calcifications occurred independently from collagen type X expression.

Limitations of the study

We aware that our research may have limitations. The first limitation of this study is that passage 1 (P1), passage 2 (P2), and passage 3 (P3) NPCs were used. Cell expansion for one or more passages could induce dedifferentiation in articular chondrocytes (72-74). This well-known phenomenon may have also played a role in our study. Consequently, dedifferentiated NPCs could respond differently from freshly isolated NPCs (P0) and therefore, future studies should determine the effect of hypertrophic induction medium, PTHrP and IHH on P0 NPCs. In **section 3.3.1.** NPCs derived from early degenerated IVDs from six canine donors were pooled in order to assess a representative degenerated NPC population. In addition, in the **sections 3.2.4.** and **3.4.2.** NPCs derived from early degenerated IVDs from six canine and/or six human donors were pooled per donor for RT-qPCR in order to prevent volume limitations.

The second limitation of this study is the problem of changing the medium at hypoxic conditions. Previous studies have shown that hypoxia could enhance the phenotype of the NPCs, which resulted in more GAG and collagen type II production (75-77). In addition, hypoxia could suppress hypertrophic differentiation of chondrocytes, while normoxia could stimulate hypertrophic differentiation (60). In the present study, the medium was replaced in a normoxic environment, for practical reasons. The abrupt change in oxygen levels from hypoxia to normoxia during medium replacement may have affected cell differentiation, especially at the periphery of the micro-aggregates. Therefore, further research under strict hypoxic conditions is necessary to confirm the obtained results.

The third limitation of this study is the low amount of donors (n=6) that were used. Due to this low amount of donors, some results were not significant despite the fact that in some cases a clear trend was visible. Therefore, future studies should be included more than 6 donors.

The fourth limitation of this study is that our study design was often based on the results in other tissues or cells because the role of PTHrP and IHH had not been investigated in healthy and degenerated IVDs yet. Possibly this design was not optimal for NPCs.

The last limitation of this study is that our 3D micro-aggregate cell culture system was not optimal to induce hypertrophy and to investigate the role of PTHrP and IHH in hypertrophic induced NPCs derived from early degenerated IVDs. Future work is needed to improve the current setup of this study or to develop a new setup that explores more explicitly the improvements and the additional study features that would be required to produce a more meaningful answer.

Overall and to conclude with, the present study highlighted the difficulties of designing a suitable cell culture setup to induce hypertrophy in NPCs derived from early degenerated IVDs to study the role of PTHrP and IHH in canine and human degenerated IVDs and therefore, the next paragraph gives a set of proposals for future directions of research.

Future directions

In the present study, we showed that our last 3D micro-aggregate cell culture model (experiment B) was still not able to induce hypertrophy in NPCs.

Illien-Jünger et al. (2016) cultured bovine NPCs and cartilaginous endplate cells in monolayer under hypoxic conditions (5% O_2) for 4 days. Their hypothesis was that calcifications and hypertrophy in the IVD are associated with advanced glycation end products (AGEs) and therefore they stimulated the NPCs and cartilaginous endplate cells with 200 µg/mL AGE-BSA medium in low glucose (1 g/L) DMEM + 1% ITS + 1% FBS + 0.2% ASAP + 0.2% Primocin. Their results demonstrated ectopic calcifications and collagen type X expression after 4 days in culture (32). Based on this, it would be interesting to study the effects of PTHrP, IHH, hypertrophic induction medium and AGE-BSA medium on NPCs derived from early degenerated canine IVDs in a 4-day monolayer culture. In this case, a next study could, for example, include the following three components: first, a next study could use a 2D cell culture system (monolayer) instead of a 3D cell culture system because in a 2D cell culture system cells grow on a flat surface and exhibit a lesser degree of structural complexity and homeostasis. It could therefore be used to determine more easily if the hypertrophic induction medium is capable of inducing hypertrophy in NPCs and which role PTHrP and IHH fulfill in NPCs derived from early degenerated IVDs. Also, monolayers consist of one cell layer and therefore, the cells have unlimited access to nutrients or other compounds from the media above and the ability to remove waste products directly into the media. In fact, this result in an optimal exchange of medium compounds. Second, the NPCs could be cultured for 4 days in chondrogenic differentiation culture medium, or hypertrophic induction medium, or AGE-BSA medium (32), or osteogenic differentiation medium (78,79) supplemented with 1% FBS, or hypertrophic induction medium / AGE-BSA medium / 1% FBS + osteogenic differentiation medium supplemented with PTHrP or IHH. FBS is considered to be a rich source of nutrients and addition to the osteogenic differentiation medium is necessary because FBS deprivation might slow down or even stop cell proliferation and increasing cell death (80). Third and last, NPCs derived from donors with and without calcified IVDs could be included in the next study to see if there is a difference between the induction of hypertrophy and calcification between the donors.

Clinical relevance

PTHrP and IHH might play a role in IVD degeneration or regeneration. If PTHrP and/or IHH plays a role in IVD degeneration, because future research also prove that PTHrP ensures less GAG production and IHH induces calcifications, then PTHrP and/or IHH have to be inhibited with, for example, PTHrP and/or IHH inhibitors.

Conversely, if future research can prove that PTHrP plays a regenerative role in the degenerated IVD, then PTHrP could be used as a therapeutic approach to slow down or even reverse IVD degeneration. For example, *PTHrP* gene therapy could be a possible approach (21). This therapy could be performed in two ways. First, the PTHrP gene could be directly injected into the NP and could affects the NPCs so that they secrete PTHrP (81). Second, the *PTHrP* gene could be transfected into cultured MSCs or NPCs, followed by transplantation of the MSCs or NPCs into the NP for sustained PTHrP production (82).

Another example of a therapeutic approach could be the direct administration of the recombinant PTHrP protein intradiscal in the IVD via injection. Recombinant PTHrP protein includes only its functional domains to which the PTHrP receptor binds. However, this therapeutic approach requires frequent injections to maintain the working concentration because after one injection PTHrP is likely to degrade and is rapidly removed (21). In addition, repeated injections are not ideal because the resulting needle puncture and injection can causes more damage in the IVD at the needle insertion site and therefore, can accelerate the degenerated process (83-88). However, the injection of therapeutics into the NP with a minimal needle size may limit damage (85).

A better example of a therapeutic approach is the use of a biomaterial based controlled release system. Biomaterials that can be used are: microspheres, hydrogels or a combination of microspheres and hydrogels (89). These biomaterials can be loaded with, for example, the *PTHrP* gene, the *PTHrP*-transfected NPCs, or the PTHrP protein and can then be injected into the IVD. Additionally, due to the very low cell density in the adult NP, cell-based therapies are a valuable addition to the biomaterial based controlled release system. MSCs are a proper cell source for cell-based therapies because they can be isolated from different tissues, expand rapidly and stably, and can be differentiate into NPCs (21,90). However, *Mueller and Tuan* reported that induction of chondrogenesis of MSCs *in vitro* is generally accompanied by unwanted hypertrophic differentiation (57,91). Therefore, combining an injection containing biomaterial loaded with PTHrP gene/protein and a cell-based therapy could have potential for a successful regenerative treatment option in degenerated IVDs. For example, the PTHrP gene or protein and MSCs could be loaded in one biomaterial and then injected into the NP.

6. Conclusion

The present study demonstrates that PTHrP and IHH play a role in IVD health and degeneration. In human IVDs, both PTHrP and IHH have a positive correlation with the IVD degeneration grade, indicating that PTHrP and/or IHH might play a role in IVD degeneration or regeneration. The results of this study indicate that PTHrP and IHH do not induce GAG deposition in canine and human NPCs. In addition, IHH seems to induce calcification in human and canine NPCs. These calcifications seem to occur independently from collagen type X expression. More *in vitro* studies are necessary to gain more direct evidence on the efficacy of PTHrP and/or IHH on the process of regeneration or degeneration in IVDs and to elucidate the role of PTHrP and IHH more clearly.

7. Acknowledgements

I would like to thank the orthopedics group for all their help. Especially, I would like to thank Drs. F.C. Bach and Dr. M.A. Tryfonidou for giving me the opportunity to do my research internship at the orthopedics group and for all the help, valuable advice, and support they gave me during my research internship.

8. References

(1) Dyce KM, Sack WO, Wensing CJG. Textbook of veterinary anatomy. Philadelphia, Pa.: Saunders; 2010.

(2) Shapiro IM, Risbud MV. The Intervertebral Disc. : Springer Vienna; 2014.

(3) Bergknut N, Smolders L, Grinwis GCM, Hagman R, Lagerstedt A, Hazewinkel HAW, et al. Intervertebral disc degeneration in the dog. Part 1: Anatomy and physiology of the intervertebral disc and characteristics of intervertebral disc degeneration. Vet J 2013;195(3):282-291.

(4) Brisson BA. Intervertebral Disc Disease in Dogs. Vet Clin N Am : Small Anim Pract 2010 9;40(5):829-858.

(5) Fingeroth J. Advances in Intervertebral Disc Disease in Dogs and Cats. : Wiley; 2015.

(6) Bach F, Willems N, Penning L, Ito K, Meij B, Tryfonidou M. Potential regenerative treatment strategies for intervertebral disc degeneration in dogs. BMC Vet Res 2014;10:3-3.

(7) Bach FC, de Vries, S A H, Krouwels A, Creemers LB, Ito K, Meij BP, et al. The species-specific regenerative effects of notochordal cell-conditioned medium on chondrocyte-like cells derived from degenerated human intervertebral discs. Eur Cell Mater 2015;30:132-46; discussion 146.

(8) Colombini A, Lombardi G, Corsi M, Banfi G. Pathophysiology of the human intervertebral disc. Int J Biochem Cell Biol 2008;40(5):837-842.

(9) Erwin WM, Hood K. The cellular and molecular biology of the intervertebral disc: A clinician's primer. J Can Chiropr Assoc 2014;58(3):246-257.

(10) Smolders L, Meij B, Onis D, Riemers F, Bergknut N, Wubbolts R, et al. Gene expression profiling of early intervertebral disc degeneration reveals a down-regulation of canonical Wnt signaling and caveolin-1 expression: implications for development of regenerative strategies. Arthritis Res Ther 2013;15(1):R23-R23.

(11) De Decker S, Gielen, Ingrid M V L, Duchateau L, Van Soens I, Bavegems V, Bosmans T, et al. Low-field magnetic resonance imaging findings of the caudal portion of the cervical region in clinically normal Doberman Pinschers and Foxhounds. Am J Vet Res 2010;71(4):428-434.

(12) da Costa R, Parent J, Partlow G, Dobson H, Holmberg D, Lamarre J. Morphologic and morphometric magnetic resonance imaging features of Doberman Pinschers with and without clinical signs of cervical spondylomyelopathy. Am J Vet Res 2006;67(9):1601-1612.

(13) HANSEN HJ. A pathologic-anatomical study on disc degeneration in dog, with special reference to the so-called enchondrosis intervertebralis. Acta Orthop Scand Suppl 1952;11:1-117.

(14) Andersson GB. Epidemiological features of chronic low-back pain. Lancet 1999;354(9178):581-585.

(15) Hohaus C, Ganey TM, Minkus Y, Meisel HJ. Cell transplantation in lumbar spine disc degeneration disease. Eur Spine J 2008;17 Suppl 4:492-503.

(16) Bach F, Zhang Y, Miranda Bedate A, Verdonschot L, Bergknut N, Creemers L, et al. Increased caveolin-1 in intervertebral disc degeneration facilitates repair. Arthritis Res Ther 2015;18:59-59.

(17) Bergknut N, Rutges, Joost P H J, Kranenburg H, Smolders L, Hagman R, Smidt H, et al. The dog as an animal model for intervertebral disc degeneration? Spine 2012;37(5):351-358.

(18) Priyadarshani P, Li Y, Yao L. Advances in biological therapy for nucleus pulposus regeneration. Osteoarthr Cartil 2016;24(2):206-212.

(19) Chung UI, Lanske B, Lee K, Li E, Kronenberg H. The parathyroid hormone/parathyroid hormone-related peptide receptor coordinates endochondral bone development by directly controlling chondrocyte differentiation. Proc Natl Acad Sci U S A 1998;95(22):13030-13035.

(20) van der Eerden, B C, Karperien M, Gevers EF, Löwik CW, Wit JM. Expression of Indian hedgehog, parathyroid hormone-related protein, and their receptors in the postnatal growth plate of the rat: evidence for a locally acting growth restraining feedback loop after birth. J Bone Miner Res 2000;15(6):1045-1055.

(21) Zhang W, Chen J, Zhang S, Ouyang H. Inhibitory function of parathyroid hormone-related protein on chondrocyte hypertrophy: the implication for articular cartilage repair. Arthritis Res Ther 2012;14(4):221-221.

(22) Wang D, Taboas JM, Tuan RS. PTHrP overexpression partially inhibits a mechanical strain-induced arthritic phenotype in chondrocytes. Osteoarthr Cartil 2011;19(2):213-221.

(23) Jiang J, Leong NL, Mung JC, Hidaka C, Lu HH. Interaction between zonal populations of articular chondrocytes suppresses chondrocyte mineralization and this process is mediated by PTHrP. Osteoarthr Cartil 2008;16(1):70-82.

(24) Bach F. The Paracrine Feedback Loop Between Vitamin D3 (1,25(OH)2D3) and PTHrP in Prehypertrophic Chondrocytes. J Cell Physiol 2014;229(12):1999-2014.

(25) Madiraju P, Gawri R, Wang H, Antoniou J, Mwale F. Mechanism of parathyroid hormone-mediated suppression of calcification markers in human intervertebral disc cells. Eur Cell Mater 2013;25:268-283.

(26) St Jacques B, Hammerschmidt M, McMahon AP. Indian hedgehog signaling regulates proliferation and differentiation of chondrocytes and is essential for bone formation. Genes Dev 1999;13(16):2072-2086.

(27) Liu Y, Liu X, Chen L, Du W, Cui Y, Piao X, et al. Targeting glioma stem cells via the Hedgehog signaling pathway. Neuroimmunol Neuroinflammation 2014;1(2):9-51.

(28) Tryfonidou MA, Hazewinkel HAW, Riemers FM, Brinkhof B, Penning LC, Karperien M. Intraspecies disparity in growth rate is associated with differences in expression of local growth plate regulators. Am J Physiol Endocrinol Metab 2010;299(6):E1044-E1052.

(29) Rutges, J P H J, Duit RA, Kummer JA, Oner FC, van Rijen MH, Verbout AJ, et al. Hypertrophic differentiation and calcification during intervertebral disc degeneration. Osteoarthr Cartil 2010;18(11):1487-1495.

(30) Handorf A, Chamberlain C, Li W. Endogenously produced Indian Hedgehog regulates TGFß-driven chondrogenesis of human bone marrow stromal/stem cells. Stem Cells Dev 2015;24(8):995-1007.

(31) Gawlitta D, van Rijen, Mattie H P, Schrijver EJM, Alblas J, Dhert WJA. Hypoxia impedes hypertrophic chondrogenesis of human multipotent stromal cells. Tissue Eng Part A 2012;18(19-20):1957-1966.

(32) Illien Jünger S, Torre OM, Kindschuh WF, Chen X, Laudier DM, Iatridis JC. AGEs induce ectopic endochondral ossification in intervertebral discs. Eur Cell Mater 2016;32:257-270.

(33) Vortkamp A, Lee K, Lanske B, Segre GV, Kronenberg HM, Tabin CJ. Regulation of rate of cartilage differentiation by Indian hedgehog and PTH-related protein. Science 1996;273(5275):613-622.

(34) Young B, Minugh Purvis N, Shimo T, St Jacques B, Iwamoto M, Enomoto Iwamoto M, et al. Indian and sonic hedgehogs regulate synchondrosis growth plate and cranial base development and function. Dev Biol 2006;299(1):272-282.

(35) Wei F, Zhou J, Wei X, Zhang J, Fleming BC, Terek R, et al. Activation of Indian hedgehog promotes chondrocyte hypertrophy and upregulation of MMP-13 in human osteoarthritic cartilage. Osteoarthr Cartil 2012;20(7):755-763.

(36) Shuang F, Zhou Y, Hou S, Zhu J, Liu Y, Zhang C, et al. Indian Hedgehog signaling pathway members are associated with magnetic resonance imaging manifestations and pathological scores in lumbar facet joint osteoarthritis. Sci Rep 2015;5:10290-10290.

(37) Amano K, Ichida F, Sugita A, Hata K, Wada M, Takigawa Y, et al. MSX2 stimulates chondrocyte maturation by controlling Ihh expression. J Biol Chem 2008;283(43):29513-29521.

(38) Mak K, Kronenberg H, Chuang P, Mackem S, Yang Y. Indian hedgehog signals independently of PTHrP to promote chondrocyte hypertrophy. Development 2008;135(11):1947-1956.

(39) Cohen-Solal M. When parathyroid hormone-related protein protects mice against osteoarthritis. IBMS BoneKEy November 2011;8:467-469.

(40) Macica C, Liang G, Nasiri A, Broadus A. Genetic evidence of the regulatory role of parathyroid hormone-related protein in articular chondrocyte maintenance in an experimental mouse model. Arthritis Rheum 2011;63(11):3333-3343.

(41) Chang J, Chang L, Hung S, Wu S, Lee H, Lin Y, et al. Parathyroid hormone 1-34 inhibits terminal differentiation of human articular chondrocytes and osteoarthritis progression in rats. Arthritis Rheum 2009;60(10):3049-3060.

(42) Chen X, Macica C, Nasiri A, Broadus A. Regulation of articular chondrocyte proliferation and differentiation by indian hedgehog and parathyroid hormone-related protein in mice. Arthritis Rheum 2008;58(12):3788-3797.

(43) Zhou J, Wei X, Wei L. Indian Hedgehog, a critical modulator in osteoarthritis, could be a potential therapeutic target for attenuating cartilage degeneration disease. Connect Tissue Res 2014;55(4):257-261.

(44) Amano K, Densmore M, Nishimura R, Lanske B. Indian hedgehog signaling regulates transcription and expression of collagen type X via Runx2/Smads interactions. J Biol Chem 2014;289(36):24898-24910.

(45) Becher C, Szuwart T, Ronstedt P, Ostermeier S, Skwara A, Fuchs Winkelmann S, et al. Decrease in the expression of the type 1 PTH/PTHrP receptor (PTH1R) on chondrocytes in animals with osteoarthritis. J Orthop Surg Res 2010;5:28-28.

(46) Brajša K. Three-dimensional cell cultures as a new tool in drug discovery. Period Biol 2016;118(1):59-65.

(47) Edmondson R, Broglie J, Adcock A, Yang L. Three-dimensional cell culture systems and their applications in drug discovery and cell-based biosensors. Assay Drug Dev Technol 2014;12(4):207-218.

(48) Fang Y, Eglen R. Three-Dimensional Cell Cultures in Drug Discovery and Development. SLAS Discov 2017;22(5):456-472.

(49) Caron MMJ, Emans PJ, Coolsen MME, Voss L, Surtel DAM, Cremers A, et al. Redifferentiation of dedifferentiated human articular chondrocytes: comparison of 2D and 3D cultures. Osteoarthr Cartil 2012;20(10):1170-1178.

(50) Urban JPG. The role of the physicochemical environment in determining disc cell behaviour. Biochem Soc Trans 2002;30(6):858-864.

(51) Bibby SRS, Urban JPG. Effect of nutrient deprivation on the viability of intervertebral disc cells. Eur Spine J 2004;13(8):695-701.

(52) Horner HA, Urban JP. 2001 Volvo Award Winner in Basic Science Studies: Effect of nutrient supply on the viability of cells from the nucleus pulposus of the intervertebral disc. Spine 2001;26(23):2543-2549.

(53) Nuttall RK, Kennedy TG. Epidermal growth factor and basic fibroblast growth factor increase the production of matrix metalloproteinases during in vitro decidualization of rat endometrial stromal cells. Endocrinology 2000;141(2):629-636.

(54) He E. The combined effects of transforming growth factor-ß and basic fibroblast growth factor on the human degenerated nucleus pulposus cells in monolayer culture. Tissue Engineering and Regenerative Medicine 2013;10(3):146-154.

(55) Koziel L, Kunath M, Kelly O, Vortkamp A. Ext1-dependent heparan sulfate regulates the range of Ihh signaling during endochondral ossification. Dev Cell 2004;6(6):801-813.

(56) Pan A, Chang L, Nguyen A, James A. A review of hedgehog signaling in cranial bone development. Front Physiol 2013;4:61-61.

(57) Mueller M, Tuan R. Functional characterization of hypertrophy in chondrogenesis of human mesenchymal stem cells. Arthritis Rheum 2008;58(5):1377-1388.

(58) Mwale F, Ciobanu I, Giannitsios D, Roughley P, Steffen T, Antoniou J. Effect of oxygen levels on proteoglycan synthesis by intervertebral disc cells. Spine 2011;36(2):E131-E138.

(59) Kauppila LI. Ingrowth of blood vessels in disc degeneration. Angiographic and histological studies of cadaveric spines. J Bone Joint Surg Am 1995;77(1):26-31.

(60) Leijten JCH, Moreira Teixeira L, Landman EBM, van Blitterswijk C, Karperien M. Hypoxia inhibits hypertrophic differentiation and endochondral ossification in explanted tibiae. PLoS ONE 2012;7(11):e49896-e49896.

(61) Brighton CT, Ray RD, Soble LW, Kuettner KE. In vitro epiphyseal-plate growth in various oxygen tensions. J Bone Joint Surg Am 1969;51(7):1383-1396.

(62) Bondeson J, Wainwright S, Hughes C, Caterson B. The regulation of the ADAMTS4 and ADAMTS5 aggrecanases in osteoarthritis: a review. Clin Exp Rheumatol 2008;26(1):139-145.

(63) Verma P, Dalal K. ADAMTS-4 and ADAMTS-5: key enzymes in osteoarthritis. J Cell Biochem 2011;112(12):3507-3514.

(64) Zheng Q, Zhou G, Morello R, Chen Y, Garcia Rojas X, Lee B. Type X collagen gene regulation by Runx2 contributes directly to its hypertrophic chondrocyte-specific expression in vivo. J Cell Biol 2003;162(5):833-842.

(65) Ding M, Lu Y, Abbassi S, Li F, Li X, Song Y, et al. Targeting Runx2 expression in hypertrophic chondrocytes impairs endochondral ossification during early skeletal development. J Cell Physiol 2012;227(10):3446-3456.

(66) Melrose J, Burkhardt D, Taylor TKF, Dillon CT, Read R, Cake M, et al. Calcification in the ovine intervertebral disc: a model of hydroxyapatite deposition disease. Eur Spine J 2009;18(4):479-489.

(67) Clark Greuel J, Connolly J, Sorichillo E, Narula N, Rapoport HS, Mohler E, et al. Transforming growth factor-beta1 mechanisms in aortic valve calcification: increased alkaline phosphatase and related events. Ann Thorac Surg 2007;83(3):946-953.

(68) Tchetina E, Mwale F, Poole AR. Distinct phases of coordinated early and late gene expression in growth plate chondrocytes in relationship to cell proliferation, matrix assembly, remodeling, and cell differentiation. J Bone Miner Res 2003;18(5):844-851.

(69) Zhao Q, Eberspaecher H, Lefebvre V, De Crombrugghe B. Parallel expression of Sox9 and Col2a1 in cells undergoing chondrogenesis. Dev Dyn 1997;209(4):377-386.

(70) Tryfonidou M, Lunstrum G, Hendriks K, Riemers F, Wubbolts R, Hazewinkel HAW, et al. Novel type II collagen reporter mice: New tool for assessing collagen 2a1 expression in vivo and in vitro. Dev Dyn 2011;240(3):663-673.

(71) Sandberg M, Vuorio E. Localization of types I, II, and III collagen mRNAs in developing human skeletal tissues by in situ hybridization. J Cell Biol 1987;104(4):1077-1084.

(72) Bekkers JEJ, Saris DBF, Tsuchida A, van Rijen, Mattie H P, Dhert WJA, Creemers L. Chondrogenic potential of articular chondrocytes depends on their original location. Tissue Eng Part A 2014;20(3-4):663-671.

(73) Veilleux NH, Yannas IV, Spector M. Effect of passage number and collagen type on the proliferative, biosynthetic, and contractile activity of adult canine articular chondrocytes in type I and II collagen-glycosaminoglycan matrices in vitro. Tissue Eng 2004;10(1-2):119-127.

(74) Kang S, Yoo S, Kim B. Effect of chondrocyte passage number on histological aspects of tissue-engineered cartilage. Biomed Mater Eng 2007;17(5):269-276.

(75) Feng G, Li L, Liu H, Song Y, Huang F, Tu C, et al. Hypoxia differentially regulates human nucleus pulposus and annulus fibrosus cell extracellular matrix production in 3D scaffolds. Osteoarthr Cartil 2013;21(4):582-588.

(76) Ni L, Liu X, Sochacki K, Ebraheim M, Fahrenkopf M, Shi Q, et al. Effects of hypoxia on differentiation from human placenta-derived mesenchymal stem cells to nucleus pulposus-like cells. Spine J 2014;14(10):2451-2458.

(77) Liu S, Song N, He J, Yu X, Guo J, Jiao X, et al. Effect of Hypoxia on the Differentiation and the Self-Renewal of Metanephrogenic Mesenchymal Stem Cells. Stem Cells Int 2017;2017:7168687-7168687.

(78) Salem O, Wang H, Alaseem A, Ciobanu O, Hadjab I, Gawri R, et al. Naproxen affects osteogenesis of human mesenchymal stem cells via regulation of Indian hedgehog signaling molecules. Arthritis Res Ther 2014;16(4):R152-R152.

(79) Nishimura I, Hisanaga R, Sato T, Arano T, Nomoto S, Ikada Y, et al. Effect of osteogenic differentiation medium on proliferation and differentiation of human mesenchymal stem cells in three-dimensional culture with radial flow bioreactor. Regenerative Therapy 2015 12;2:24-31.

(80) Nonnis S, Maffioli E, Zanotti L, Santagata F, Negri A, Viola A, et al. Effect of fetal bovine serum in culture media on MS analysis of mesenchymal stromal cells secretome. EuPA Open Proteomics 2016 3;10:28-30.

(81) Steinert A, Nöth U, Tuan R. Concepts in gene therapy for cartilage repair. Injury 2008;39 Suppl 1:S97-113.

(82) Xian C, Foster B. Repair of injured articular and growth plate cartilage using mesenchymal stem cells and chondrogenic gene therapy. Curr Stem Cell Res Ther 2006;1(2):213-229.

(83) Korecki C, Costi J, Iatridis J. Needle puncture injury affects intervertebral disc mechanics and biology in an organ culture model. Spine 2008;33(3):235-241.

(84) Iatridis J, Hecht A. Commentary: Does needle injection cause disc degeneration? News in the continuing debate regarding pathophysiology associated with intradiscal injections. Spine J 2012;12(4):336-338.

(85) Martin J, Gorth D, Beattie E, Harfe B, Smith L, Elliott D. Needle puncture injury causes acute and long-term mechanical deficiency in a mouse model of intervertebral disc degeneration. J Orthop Res 2013;31(8):1276-1282.

(86) Nassr A, Lee J, Bashir R, Rihn J, Eck J, Kang J, et al. Does incorrect level needle localization during anterior cervical discectomy and fusion lead to accelerated disc degeneration? Spine 2009;34(2):189-192.

(87) Carragee E, Don A, Hurwitz E, Cuellar J, Carrino J, Herzog R. 2009 ISSLS Prize Winner: Does discography cause accelerated progression of degeneration changes in the lumbar disc: a ten-year matched cohort study. Spine 2009;34(21):2338-2345.

(88) Michalek A, Buckley M, Bonassar L, Cohen I, Iatridis J. The effects of needle puncture injury on microscale shear strain in the intervertebral disc annulus fibrosus. Spine J 2010;10(12):1098-1105.

(89) Schutgens EM, Tryfonidou MA, Smit TH, Öner FC, Krouwels A, Ito K, et al. Biomaterials for intervertebral disc regeneration: past performance and possible future strategies. Eur Cell Mater 2015;30:210-231.

(90) Choi H, Johnson Z, Risbud M. Understanding nucleus pulposus cell phenotype: a prerequisite for stem cell based therapies to treat intervertebral disc degeneration. Curr Stem Cell Res Ther 2015;10(4):307-316.

(91) Chen S, Fu P, Cong R, Wu H, Pei M. Strategies to minimize hypertrophy in cartilage engineering and regeneration. Genes Dis 2015;2(1):76-95.

9. Appendix

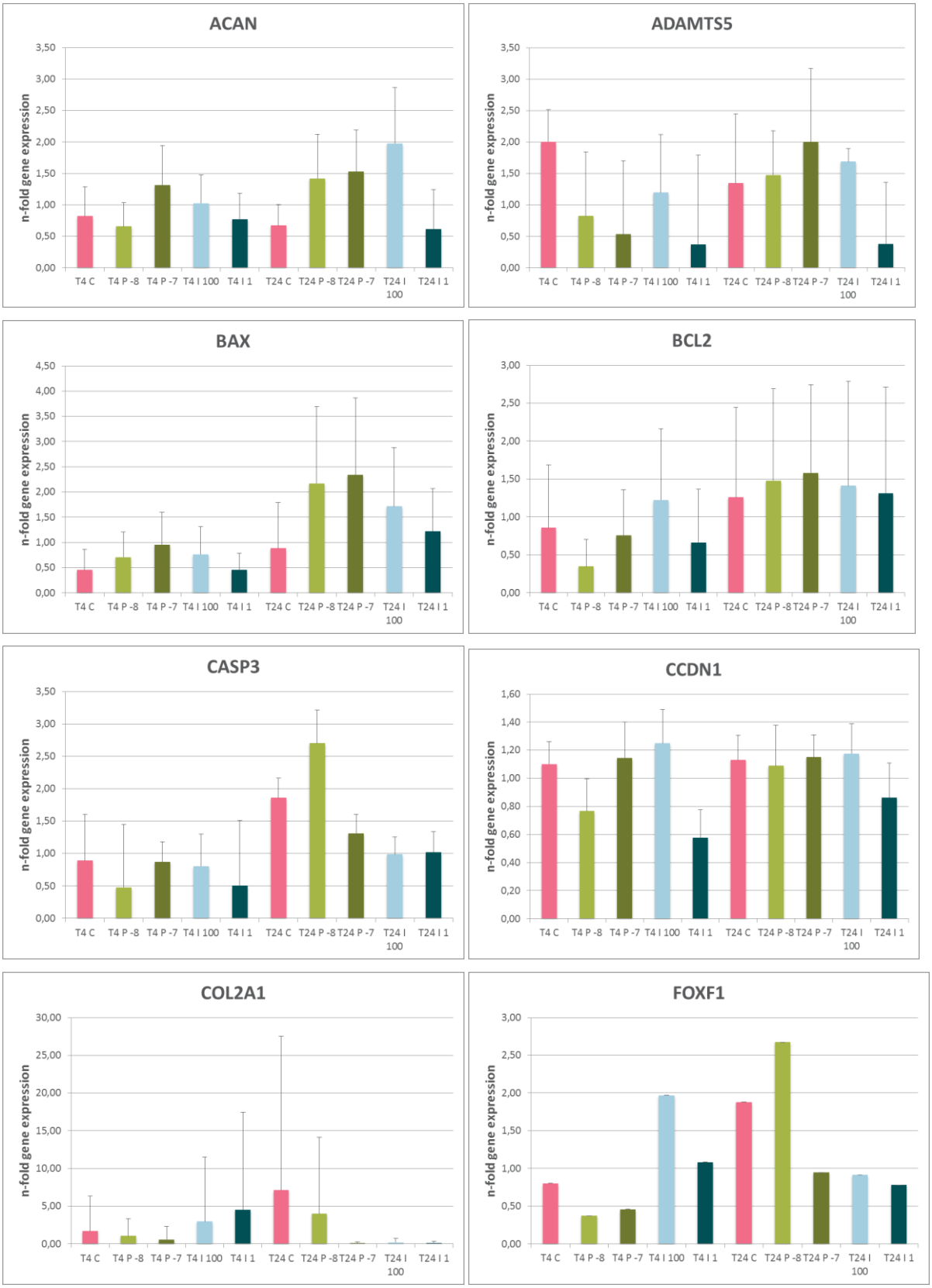

Figure 23. The gene expression levels of the *ACAN, ADAMTS5, BAX, BCL2, CASP3, CCDN1, COL2A1, and FOXF1* genes in canine nucleus pulposus cell micro-aggregates after 4 and 24 hours of culturing in hypoxia (5% O_2, 5% CO_2, 37 °C). n=6 in duplo per culture condition.

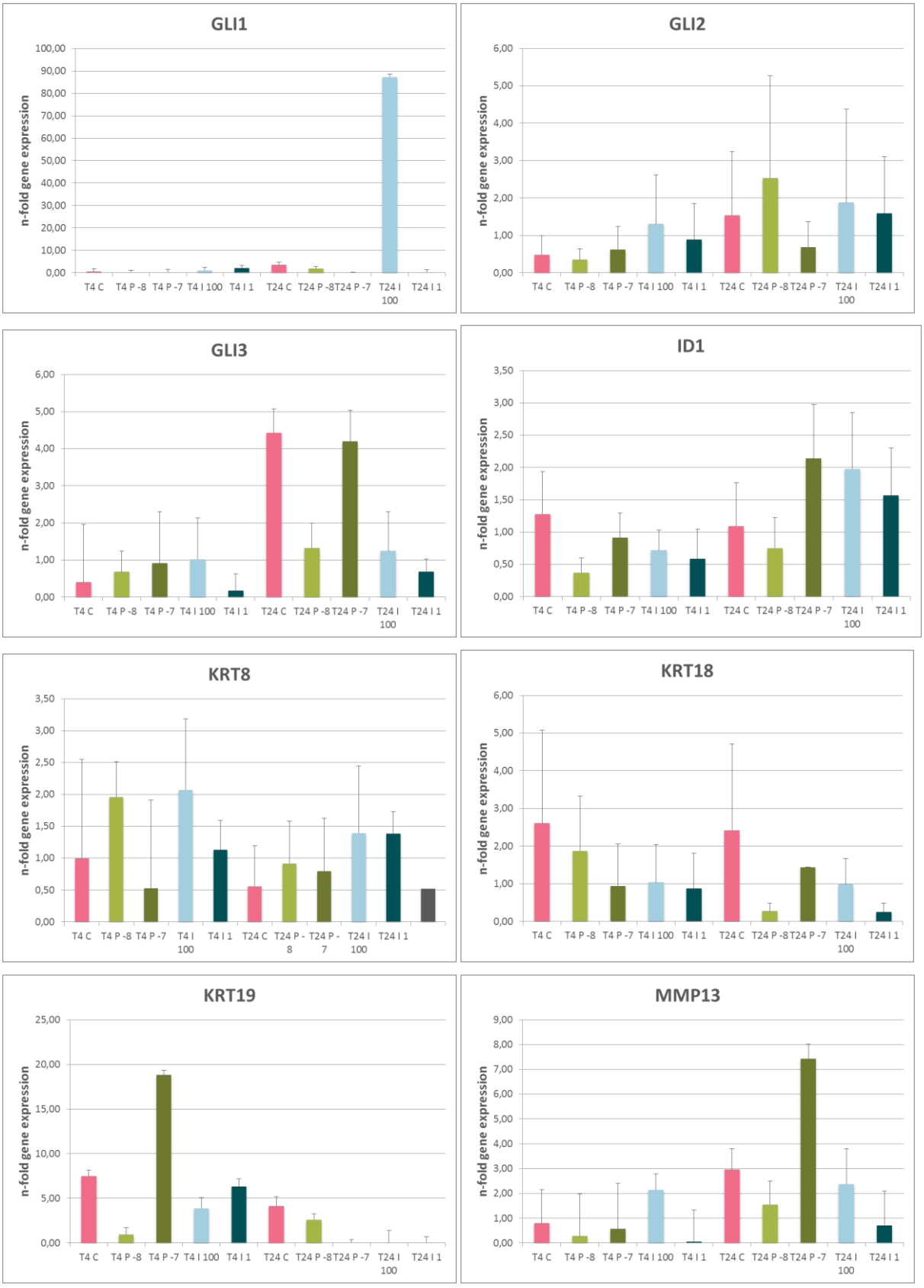

Figure 24. The gene expression levels of the *GLI1, GLI2, GLI3, ID1, KRT8, KRT18 ,KRT19, and MMP13* genes in canine nucleus pulposus cell micro-aggregates after 4 and 24 hours of culturing in hypoxia (5% O_2). n=6 in duplo per culture condition.

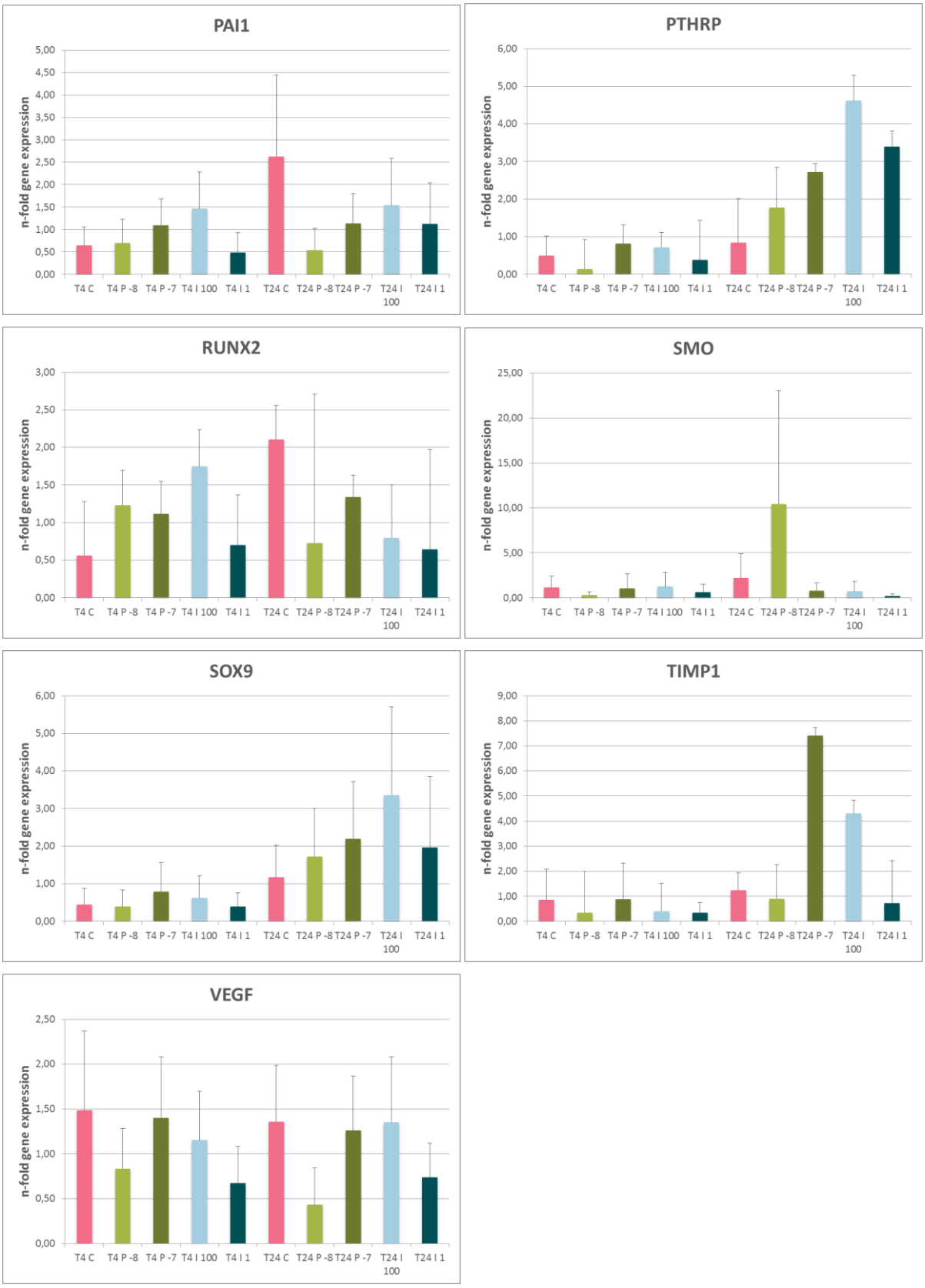

Figure 25. The gene expression levels of the *PAI1, PTHrP, RUNX2, SMO, SOX9, TIMP1, and VEGF* genes in canine nucleus pulposus cell micro-aggregates after 4 and 24 hours of culturing in hypoxia (5% O_2). n=6 in duplo per culture condition.

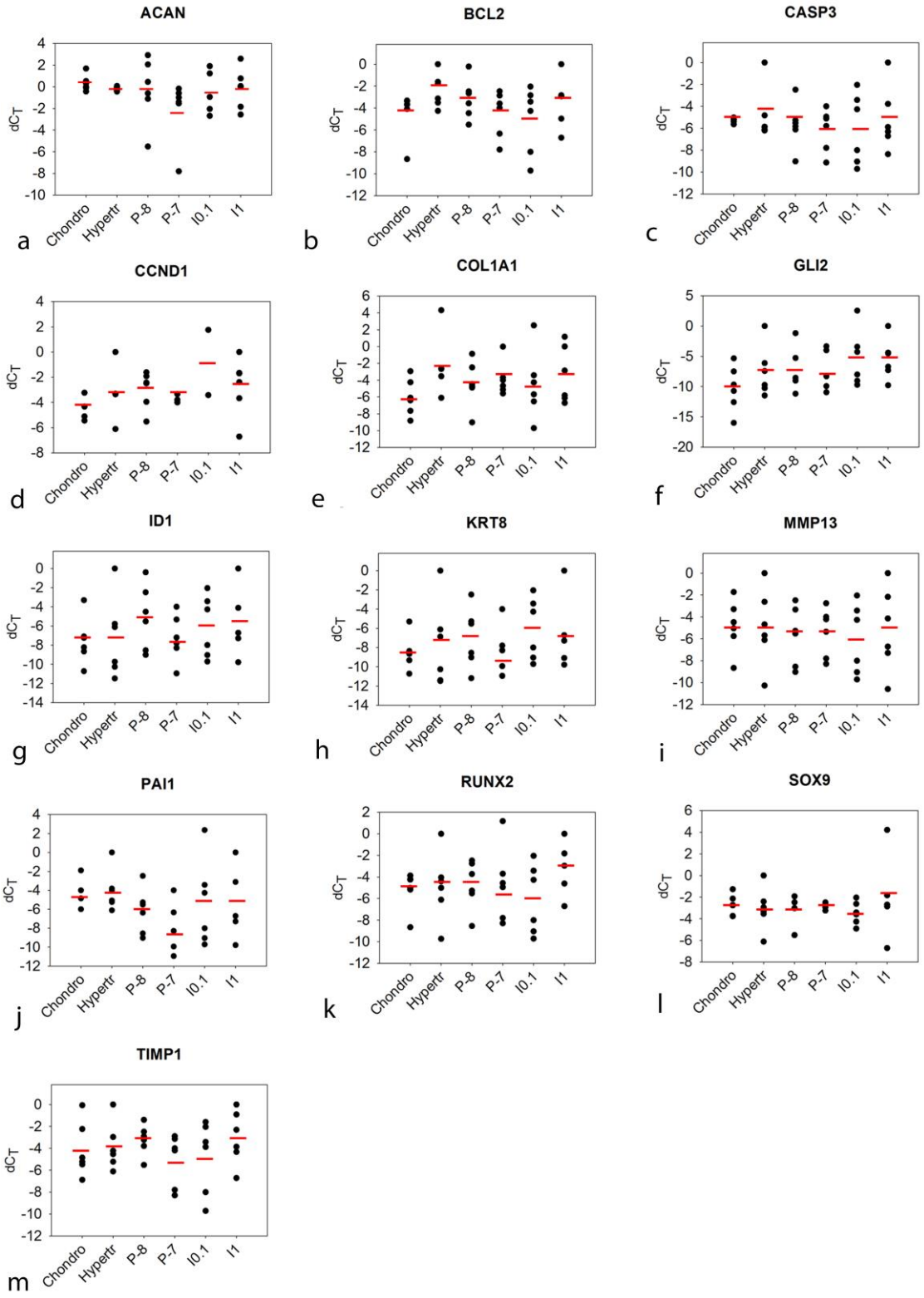

Figure 26. The ΔC_T-values, which are relative measures of the concentration of the target gene in the Real-Time quantitative Polymerase Chain Reaction analysis, of the *ACAN, BCL2, CASP3, CCND1, COL1A1, GLI2, ID1, KRT8, MMP13, PAI1, RUNX2, SOX9, and TIMP1* genes in canine nucleus pulposus cell micro-aggregates at day 35 in normoxia (21% O_2). Each black dot represents one particular canine donor and each red line represents the mean of the 6 canine donors in one specific culture condition. *n*=6 in duplo per culture condition; * $p<0.05$; ** $p<0.01$; *** $p<0.001$.

	Endplate	Nucleus Pulposus	Annulus Fibrosus	Blood vessels	Endothelial cells	Osteoblasts	Osteoclasts	Growth plate cartilage cells (reserve, proliferative, hypertrophic)
PTHrP	+ [21] Mouse, rat *Note 14*	- [21] Mouse, rat *Note 14*	- [21] Mouse, rat *Note 14*	+ [2,3] Human PTHrP acts on vascular smooth muscle cells	+ [2, 21] Mouse, rat In vascular[2] and coronary[21] endothelial cells	+ [1, 12] Human	- [2] / + [12, 13] Human, rabbit, mouse *Note 5,6,21*	+ [24, 25] Human, rat In peri-articulair proliferating chondrocytes *Note 14,19*
PTHR1	+ [20] Mouse *Note 12,13*	+ [20] Mouse *Note 12*	+ [20] Mouse *Note 12,13*	+ [2] Human In vascular smooth muscle cells *Note 1*	+ [21] Mouse, rat *Note 15*	+ [1,4,5,7,8,17] Human	- [5,6,7] Human	+ [10,15, 17, 20, 24, 25] Mouse, rat In prehypertrophic and hypertrophic chondrocytes *Note 8,12,19*
IHH	+ [10] Mouse *Note 16*	- [10] Mouse *Note 16*	- [10] Mouse *Note 16*	+ [19] Human *Note 10,11*	+ [9] Mouse *Note 10*	+ [11,12,16, 27] Human, mouse, rat *Note 3,19,20*	- [12] Human *Note 5*	+ [10,15, 24, 25, 26, 27] Human, mouse, rat In prehypertrophic and hypertrophic chondrocytes *Note 7,19,20*
Ptc	- [16] Mouse *Note 9*	+ [10] Mouse *Note 2,9*	- [16] Mouse *Note 9*	**Unknown**	+ [22] Human In umbilical vein *Note 17*	+ [12,16] Human, mouse *Note 4*	- [12] Human *Note 5*	+ [24] Rat *Note 19*

Smo	**Unknown**	**Unknown**	**Unknown**	**+** [18] Human *Note 10*	**+** [18, 23] Human *Note 10,18*	**+** [16] Mouse	**Unknown**	**+** [24] Rat *Note 19*

Table 8. The localization of the expression of Parathyroid hormone-related peptide (PTHrP), PTHrP receptor type 1 (PTHR1), Indian Hedgehog (IHH), and the receptors of IHH: Patched (Ptc) and Smoothened (Smo).

- ***Note 1****: PTHrP is produced in vascular endothelial cells and acts on vascular smooth muscle cells*[2]*, so probably vascular smooth muscle cells contain the PTHrP receptor / PTHR1.*
- ***Note 2****: Ptc protein was expressed in the developing nucleus pulposus (14.5 days post conception in the mouse embryo until birth)* [10]*.*
- ***Note 3****: At 3 weeks after fracture in adult rat femora, some of the osteoblasts close to the endochondral ossification front were also stained positive for Indian hedgehog protein.*
- ***Note 4****: PTHrP, IHH, and Ptc showed positive immunostaining in osteoblasts in the bone-forming area.*[12]
- ***Note 5****: In the bone resorption site, PTHrP was immunolocalized in osteoclasts, whereas IHH and Ptc were not.*[12]
- ***Note 6****: Active osteoclasts at bone resorption sites (in the rabbit and mouse) expressed both mRNA and protein for PTHrP. However, occasional osteoclasts were found to be negative for PTHrP expression. Localization of PTHrP was also demonstrated in osteoclast-like cells of human giant cell tumors from bone. Finally, mRNA and protein for PTHrP were expressed in osteoclasts in sections of bone or joints from patients with Paget's disease, rheumatoid arthritis, and osteoarthritis.*[13]
- ***Note 7****: During mouse embryonic development, IHH expression is first detected at embryonic stage 11.5 in early cartilaginous chondrocytes. During hypertrophic differentiation IHH expression becomes restricted to the prehypertrophic chondrocytes.*[10]
- ***Note 8****: PTHR1 is expressed at low levels throughout the growth plate. PTHR1 is expressed at high levels in the transition zone from proliferating into hypertrophic chondrocytes.* [10]
- ***Note 9****: DiPaola et al. (2005) identify the expression pattern of Ptc protein, Smo mRNA and IHH mRNA. Ptc protein was only expressed in the developing nucleus pulposus and not in the annulus fibrosus and vertebral endplate.* [10]
- ***Note 10****: Only endothelial cells of blood vessels were positive for the expression of both Smo and Ihh.*[18]
- ***Note 11****: Pancreatic cancer cells demonstrated IHH immunoreactivity. The stroma surrounding this cancer showed weak IHH immunoreactivity in the fibroblasts and smooth muscle cells of the blood vessels. This weak IHH immunoreactivity was visible in approximately 20% of the cases.*[19]
- ***Note 12****: PTHR1 expression was visible in the growth plate, endplate, annulus fibrosus and nucleus pulposus of two-month-old mouse IVDs.*[20]
- ***Note 13****: PTHR1 expression was visible in the endplate and at times in the annulus fibrosus of postnatal mouse IVDs.* [20]
- ***Note 14****: PTHrP expression in the IVD was off at 1 week, appeared at 2 weeks but only in the endplate, where its expression increased during the vertebral growth plate. The annulus fibrosus and the nucleus pulposus were negative for PTHrP.*[21]
- ***Note 15****: Ventricular endothelial cells can express PTHR1.*[21]
- ***Note 16****: IHH mRNA was only expressed by chondrocytes of the vertebral bodies and later becomes restricted to the endplate of the IVDs.*[10]
- ***Note 17:*** *IHH inhibits Ptc in endothelial cells.*[22]
- ***Note 18****: Smo was highly expressed in endothelial cells of synovial tissue from active rheumatoid arthritis patients.*[23]
- ***Note 19****: The IHH, Ptc, Smo, PTHrP and PTHR1 mRNAs were detected in postnatal growth plate tissue isolated from female and male rats that were 1, 4, 7, and 12 weeks of age.*[24]
- ***Note 20:*** *In mouse, IHH expression has been detected in prehypertrophic chondrocytes and osteoblasts. In rats, IHH has been detected in the tibial growth plates at 4 and 12 weeks of age; similarly, in humans, IHH expression has been detected in growth plates with the highest expression during the early stages of puberty.*[27]
- ***Note 21****: Fibroblasts, osteoclasts and adipocytes are cell types that did not produce PTHrP but respond to PTHrP.*[2]

10. Attended courses

- **'Academic writing'** instructed by Pamela Zak
- **Private English Lessons** instructed by Taylor Krohn

11. Attended congresses

- **'Veterinary Science Day' 2016**
- **'European Veterinary Conference Voorjaarsdagen' 2017**, attended with a Poster presentation named; '*The expression of Parathyroid hormone-related peptide and Indian Hedgehog in intervertebral disc degeneration'*
- **Annual meeting 'Nederlandse Vereniging voor Matrix Biologie' 2017**, attended with a Poster presentation named; '*The role of Parathyroid hormone-related peptide and Indian Hedgehog in intervertebral disc degeneration'*